



# Structural interfaces in linear elasticity. Part II: Effective properties and neutrality

K. Bertoldi, D. Bigoni\*, W.J. Drugan<sup>1</sup>

*Dipartimento di Ingegneria Meccanica e Strutturale, Università di Trento, Via Mesiano 77, I-38050 Trento, Italy*

Received 9 February 2006; received in revised form 13 June 2006; accepted 15 June 2006

---

## Abstract

The model of structural interfaces developed in Part I of this paper allows us to analytically attack and solve different problems of stress concentration and composites. In particular, (i) new formulae are given for effective properties of composite materials containing dilute suspensions of (randomly oriented) reinforced elliptical voids or inclusions; (ii) a new definition is proposed for inclusion neutrality (to account for the fact that the matrix is always ‘overstressed’, and thus non-neutral in a classical sense, at the contacts with the interfacial structure), which is shown to provide interesting stress optimality conditions. More generally, it is shown that the incorporation of an interfacial structure at the contact between two elastic solids exhibits properties that cannot be obtained using the more conventional approach of the zero-thickness, linear interface. For instance: contrary to the zero-thickness interface, both bulk and shear effective moduli can be optimized for a structural interface; effective properties higher than those possible with a perfect interface can be attained with a structural interface; and neutrality holds with a structural interface for a substantially broader range of parameters than for a zero-thickness interface.

© 2006 Elsevier Ltd. All rights reserved.

*Keywords:* Structural interfaces; Composite materials; Neutral inclusions; Reinforced cracks; Stress intensity factors

---

---

\*Corresponding author. Tel.: +39 0461 882 507; fax: +39 0461 882 599.

*E-mail addresses:* [katia.bertoldi@ing.unitn.it](mailto:katia.bertoldi@ing.unitn.it) (K. Bertoldi), [davide.bigoni@ing.unitn.it](mailto:davide.bigoni@ing.unitn.it) (D. Bigoni), [drugan@engr.wisc.edu](mailto:drugan@engr.wisc.edu) (W.J. Drugan).

*URL:* <http://www.ing.unitn.it/~bigoni>.

<sup>1</sup>Permanent address: Department of Engineering Physics, 1500 Engineering Drive, University of Wisconsin-Madison, Madison, WI, 53706, USA.

## 1. Introduction

The mechanical properties of the interphase, which separates inclusions from the matrix in composite materials, have been demonstrated to play an important role in the overall behavior of the composite.<sup>2</sup> Often the interphase is modelled as a surface separating two materials, across which displacements may be discontinuous, but this discontinuity is (linearly or nonlinearly) related to tractions. A more realistic model—which takes account of the actual interfacial microstructure—is obtained through the concept of a structural interface, developed in Part I of this paper. The focus of the present Part II is to investigate the role of this microstructure on the mechanical properties of composite (fiber- and particulate-reinforced) materials, always under the assumptions of two-dimensional linear elasticity. These can be quantified through investigation of: (i) stiffness, and (ii) strength. In particular,

- i) Stiffness is quantified (in Section 2) by finding the effective properties of a material containing a dilute suspension of randomly oriented elliptical inclusions connected to the matrix via a structural interface. It is shown that there are geometries of the interfacial structure yielding optimal properties in terms of shear and bulk stiffness. We determine for the first time the effective properties of a dilute suspension of randomly oriented fiber-reinforced elliptical voids, showing the strong effect of the fibers. In addition, we show that the effective properties tend to those of the matrix for a certain distribution of *inclined* fibers. In this sense, a reinforced void can be designed that leaves the stiffness of the matrix unchanged.
- ii) Strength is addressed (in Section 3) in the following way. A neutral inclusion, i.e. an inclusion which does not perturb the ambient stress/strain fields, is considered optimal from the point of view of strength, since it eliminates stress concentrations. It is shown that a circular inclusion coated by a continuous structural interface is neutral under both shear and equal biaxial tension, for a far broader material parameter range than for the linear interface analyzed by Ru (1998). In addition, the notion of weak neutrality, based on energetic arguments and more general than the concept of neutrality usually employed (e.g. Ru, 1998; Milton and Serkov, 2001), is introduced. This is useful for analyzing discrete interfacial structures and reveals that interfacial structures can be tailored to produce: (a) weakly neutral elliptical inclusions coated by a discrete structural interface under remote shear but not under equal biaxial tension; (b) weakly neutral circular inclusions coated by a discrete structural interface under both shear and equal biaxial tension separately.

---

<sup>2</sup>In particular, to quote some among many contributions, Walpole (1978) showed that a thin coating on an inclusion strongly influences the stress fields; Benveniste (1985), Achenbach and Zhu (1989, 1990), Hashin (1990, 1991a, b) obtained expressions for the effective moduli; Levy (1996) introduced a nonlinear separation mechanism in the problem of effective transverse bulk response of a composite; Hashin (2002) derived by a Taylor expansion method imperfect interface conditions which are equivalent to the effect of a thin elastic interface.

## 2. The effective properties of a dilute composite containing inclusions with structural interfaces

It is shown in this section that analytical expressions can be found for the effective elastic properties of a dilute suspension of randomly oriented reinforced elliptical voids and elliptical inclusions, connected to an elastic matrix by structural interfaces. The effective properties of the composite are shown to depend strongly on the geometry and stiffness of the interfacial structure, a finding allowing design of structural interfaces to obtain extreme properties of composites.

We refer to the volume averaged stress  $\bar{\sigma}$  and strain  $\bar{\epsilon}$

$$\bar{\sigma} = \frac{1}{V} \int_V \sigma \, dV = \frac{1}{V} \int_{\partial S} (\sigma \mathbf{n} \otimes \mathbf{x}) \, dS, \quad \bar{\epsilon} = \frac{1}{V} \int_V \epsilon \, dV = \frac{1}{V} \int_{\partial S} (\mathbf{u} \otimes \mathbf{n})_{\text{Sym}} \, dS, \quad (1)$$

(in which the suffix Sym denotes the symmetric part of a tensor) so that the effective elastic Lamé constants  $\bar{\lambda}$ ,  $\bar{\mu}$  and two-dimensional bulk modulus  $\bar{K}$  are introduced as

$$\bar{\sigma} = \bar{\lambda}(\text{tr} \bar{\epsilon}) \mathbf{I} + 2\bar{\mu} \bar{\epsilon} = \bar{K}(\text{tr} \bar{\epsilon}) \mathbf{I} + 2\bar{\mu} \text{dev} \bar{\epsilon}, \quad (2)$$

where dev and tr are the operators taking the deviatoric part and the trace of a tensor and the elastic constants appearing in Eq. (2) are related as

$$\bar{K} = \bar{\mu} + \bar{\lambda} = \frac{2\bar{\mu}}{\bar{\kappa} - 1}. \quad (3)$$

This section is organized as follows. First, the effective moduli of a dilute suspension of circular inclusions coated with a continuous double Warren structural interface (of the type analyzed in Part I, Section 4 of this paper—see Fig. 1) are obtained as simple analytical expressions. Second, discrete interfacial structures are analyzed, reinforcing randomly oriented elliptical voids and inclusions.

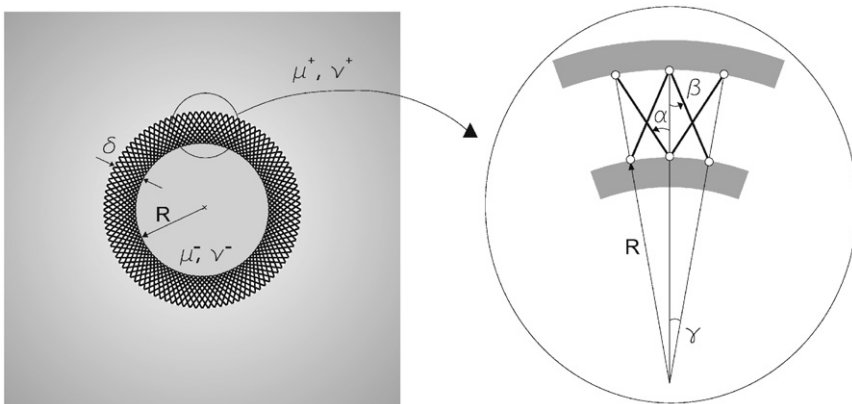


Fig. 1. Circular inclusion of radius  $R$  coated with a continuous double Warren structure of thickness  $\delta$ .

### 2.1. Dilute suspension of circular inclusions connected to the matrix by a continuous structural interface

Let us consider a dilute suspension of circular inclusions of radius  $R$  connected to an infinite matrix by a continuous double Warren truss structure of thickness  $\delta$  (Fig. 1).

When a remote uniaxial stress  $\sigma_{11}^\infty$  is applied to the matrix, substitution of the complex potentials solution (given by Eq. (49) in Part I of this article) into Eqs. (1) and neglecting terms of  $O(f^2)$  yields

$$\begin{aligned}\bar{\sigma}_{xx} &= \sigma_{11}^\infty + \frac{F_m - B_m}{(R + \delta)^2} \sigma_{11}^\infty f, \\ \bar{\sigma}_{yy} &= \frac{F_m + B_m}{(R + \delta)^2} \sigma_{11}^\infty f, \quad \bar{\sigma}_{xy} = 0, \\ \bar{\varepsilon}_{xx} &= \frac{(1 + \kappa^+) \sigma_{11}^\infty}{8\mu^+} + \frac{B_m \kappa^+ - F_m}{2(R + \delta)^2 \mu^+} \sigma_{11}^\infty f, \\ \bar{\varepsilon}_{yy} &= \frac{(\kappa^+ - 3) \sigma_{11}^\infty}{8\mu^+} - \frac{B_m \kappa^+ + F_m}{2(R + \delta)^2 \mu^+} \sigma_{11}^\infty f, \quad \bar{\varepsilon}_{xy} = 0,\end{aligned}\quad (4)$$

where  $f = (R + \delta)^2 / r^2$  is the inclusion volume fraction, and the coefficients  $B_m$ ,  $F_m$  are given by Eqs. (51) in Part I of this article. Introduction of (4) into Eq. (2) yields

$$\frac{\bar{\mu}}{\mu^+} = 1 - \frac{2B_m(\kappa^+ + 1)}{(R + \delta)^2} f, \quad \frac{\bar{K}}{K^+} = 1 + \frac{2F_m(\kappa^+ + 1)}{(R + \delta)^2(\kappa^+ - 1)} f. \quad (5)$$

In the limit case of a zero-thickness linear interface (obtained by setting  $\gamma = c\delta$  and taking the limit as  $\delta \rightarrow 0$ ), the coefficients  $B_m$  and  $F_m$  are given in Eqs. (54) in Part I of this article, so that the effective properties of the composite are the same as those given by Thorpe and Jasiuk (1992) and Bigoni et al. (1998).

The effective moduli for an inclusion volume fraction of 0.1 are plotted in Figs. 2–4 as a function of the fiber inclination  $\alpha$ . Matrix and inclusion are characterized by  $\mu^-/\mu^+ = 10$  in Fig. 2 and  $\mu^-/\mu^+ = 0.1$  in Fig. 3, while both cases are considered in Fig. 4 (in all cases  $v^- = v^+ = 1/3$ ). Different values of the dimensionless fiber compliance parameter  $\Lambda_c = 2\mu^+ / [(\kappa^+ + 1)kR]$  (see Eq. (65) in Part I of this article) have been considered and geometries defined by  $\delta/R = \{0, 0.25, 0.5, 1\}$ . Note that for the limiting case of a linear zero-thickness interface, when  $\alpha = 0$  the tractions at the interface are given by

$$\sigma_{rr} = 2k \llbracket u_r \rrbracket, \quad \sigma_{r\theta} = 0, \quad (6)$$

while when  $\alpha \rightarrow \pi/2$  they become

$$\sigma_{rr} = 0, \quad \sigma_{r\theta} = 2k \llbracket u_\theta \rrbracket. \quad (7)$$

In the case of a perfect interface, the averaged properties reduce to the well-known results (see, for instance, Willis, 1982)

$$\frac{\bar{\mu}}{\mu^+} = 1 + f \frac{(1 + \kappa^+)(\mu^- - \mu^+)}{\kappa^+ \mu^- + \mu^+}, \quad \frac{\bar{K}}{K^+} = 1 + f \frac{(1 + \kappa^+)[\mu^-(\kappa^+ - 1) - \mu^+(\kappa^- - 1)]}{(\kappa^+ - 1)(2\mu^- + \mu^+(\kappa^- - 1))}, \quad (8)$$

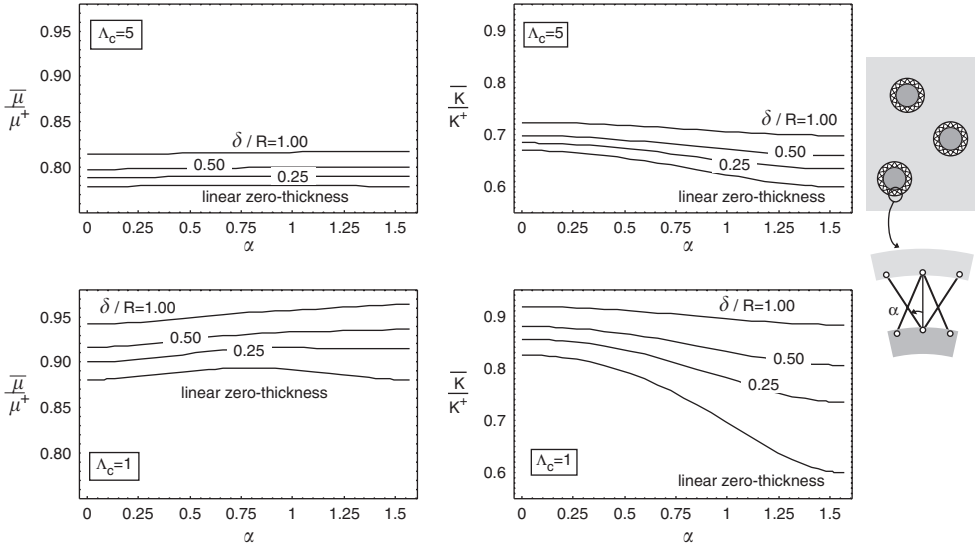


Fig. 2. Effective shear modulus  $\bar{\mu}$  (left) and 2D bulk modulus  $\bar{K}$  (right) (normalized by  $\mu^+$  and  $K^+$ , respectively) of a dilute suspension ( $f = 0.1$ ) of circular elastic inclusions of radius  $R$  connected to the matrix by a continuous double Warren truss structure with thickness  $\delta$  and fibers' inclination  $\alpha$ . The inclusions are stiffer than the matrix ( $\mu^-/\mu^+ = 10$ ) and  $\nu^+ = \nu^- = \frac{1}{3}$ , whereas the interfacial compliance is  $A_c = 5$  (upper part) and  $A_c = 1$  (lower part).

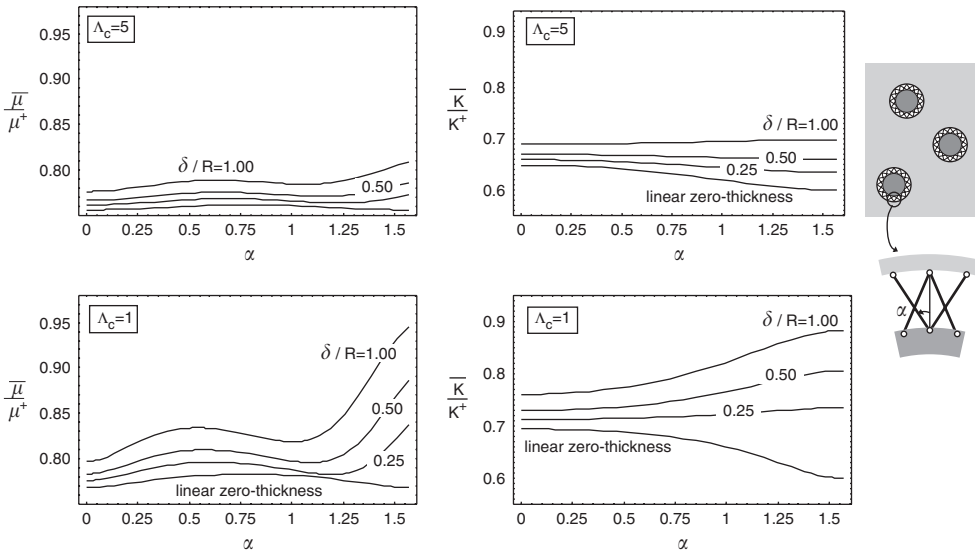


Fig. 3. Effective shear modulus  $\bar{\mu}$  (left) and 2D bulk modulus  $\bar{K}$  (right) (normalized by  $\mu^+$  and  $K^+$ , respectively) of a dilute suspension ( $f = 0.1$ ) of circular elastic inclusions of radius  $R$  connected to the matrix by a continuous double Warren truss structure with thickness  $\delta$  and bars inclination  $\alpha$ . The matrix is stiffer than the inclusions ( $\mu^-/\mu^+ = 0.1$ ) and  $\nu^+ = \nu^- = \frac{1}{3}$ , whereas the interfacial compliance is  $A_c = 5$  (upper part) and  $A_c = 1$  (lower part).

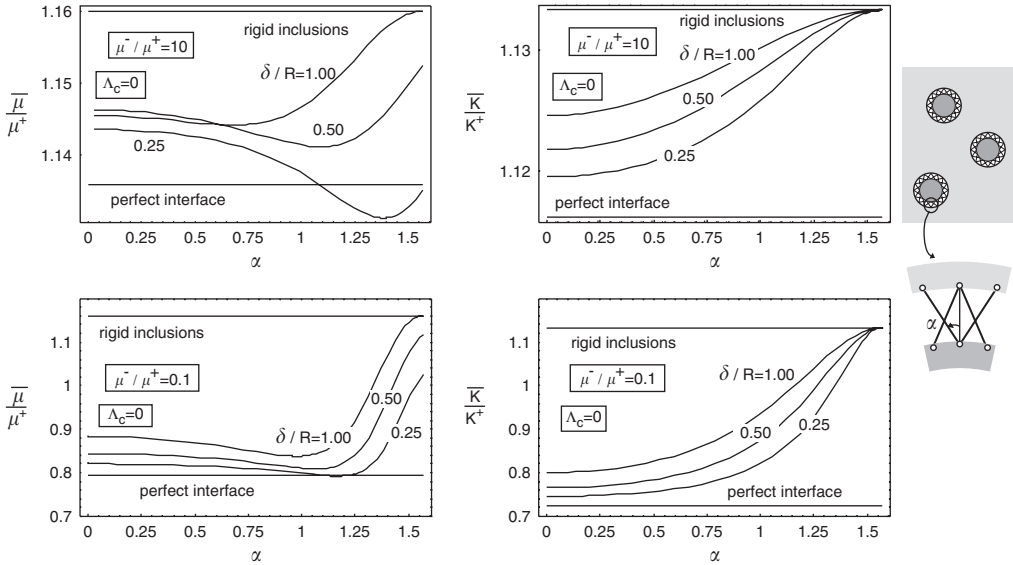


Fig. 4. Effective shear modulus  $\bar{\mu}$  (left) and 2D bulk modulus  $\bar{K}$  (right) (normalized by  $\mu^+$  and  $K^+$ , respectively) of a dilute suspension ( $f = 0.1$ ) of circular elastic inclusions of radius  $R$  connected to the matrix by a continuous double Warren truss structure with thickness  $\delta$  and bars inclination  $\alpha$ . Both inclusions stiffer than the matrix ( $\mu^-/\mu^+ = 10$ , upper part) and inclusions less stiff than the matrix ( $\mu^-/\mu^+ = 0.1$ , lower part) are considered, whereas  $\nu^+ = \nu^- = \frac{1}{3}$  and the bars are rigid ( $A_c = 0$ ). Two perfect interface results are also plotted: one for the same  $\mu^-/\mu^+$  ratio as for the structural interface cases, and one for rigid inclusions.

so that we get  $\bar{\mu}/\mu^+ = 1.135$ ,  $\bar{K}/K^+ = 1.116$  for  $\mu^-/\mu^+ = 10$  and  $\bar{\mu}/\mu^+ = 0.794$ ,  $\bar{K}/K^+ = 0.723$  for  $\mu^-/\mu^+ = 0.1$ , values shown in Fig. 4, where bars having an infinite stiffness (i.e.  $A_c = 0$ ) are considered.

We conclude from Figs. 2–4 that

- While it is obvious that increasing (decreasing) the bars' stiffness, the averaged bulk and shear moduli of the composite increase (decrease), it may be surprising to note that *for inclusions less stiff than the matrix, the averaged moduli may be stiffer than the matrix moduli, if the interfacial structure is stiff enough* (Fig. 4). This effect cannot be obtained with a linear, zero-thickness interface, which always decreases the stiffness of the composite material.
- As a function of the bars' inclination  $\alpha$ , the averaged bulk modulus has two stationary points, at  $\alpha = 0$  and  $\alpha = \pi/2$ . Moreover,  $\alpha = 0$  corresponds to a maximum for  $\bar{K}$  if

$$A_c > \frac{\delta\mu^+(2R + \delta)(\kappa^- - 1)}{\mu^- R^2(\kappa^+ + 1)}. \quad (9)$$

- For a zero-thickness linear interface, Eq. (9) yields the condition  $\alpha = 0$  (corresponding to null tangential stiffness  $k_\theta = 0$ ) for the maximum averaged bulk modulus, while the averaged shear modulus attains a maximum for  $\alpha = \pi/4$  (corresponding to equal tangential and radial stiffnesses  $k_r = k_\theta = k$ ). Therefore, *for a zero-thickness linear interface it is not possible to maximize both the bulk and the shear moduli of the composite*

material. It is clear from Figs. 3–4 that *this is not true if the inclusions are connected to the matrix through a structural interface: in fact, a structural interface with bars characterized for instance by  $A_c = 1$  and inclination  $\alpha = \pi/2$  allows us to maximize both the bulk and the shear moduli of the composite material* (Fig. 5).

## 2.2. Dilute suspension of randomly oriented elliptical voids and inclusions reinforced by discrete structures

A dilute suspension of randomly oriented elliptical voids reinforced by an arbitrary distribution of bars or reinforced by a structural interface enclosing an elliptical inclusion, so that there are  $N$  junction regions on the boundary of each void, is now considered.

The averaged stress and strain can be determined by using Eqs. (1), with reference to a circular contour of radius  $r$ , centered at the center of the elliptical void. To this purpose, we need the leading-order terms of the displacements and tractions, calculated on the large circle having  $r \gg R$ . These fields can be obtained by using the resultants  $P_k$  and  $S_k$  (in the radial and tangential directions, respectively), applied at the center of the  $k$ th junction region. We will determine now (employing the complex potentials given by Eq. (32) in Part I of this paper) the leading-order large- $r$  terms of the displacement and stress fields, assuming that the void's boundary is loaded by  $N$  concentrated forces of tangential and normal components  $S_k$  and  $P_k$ , respectively.

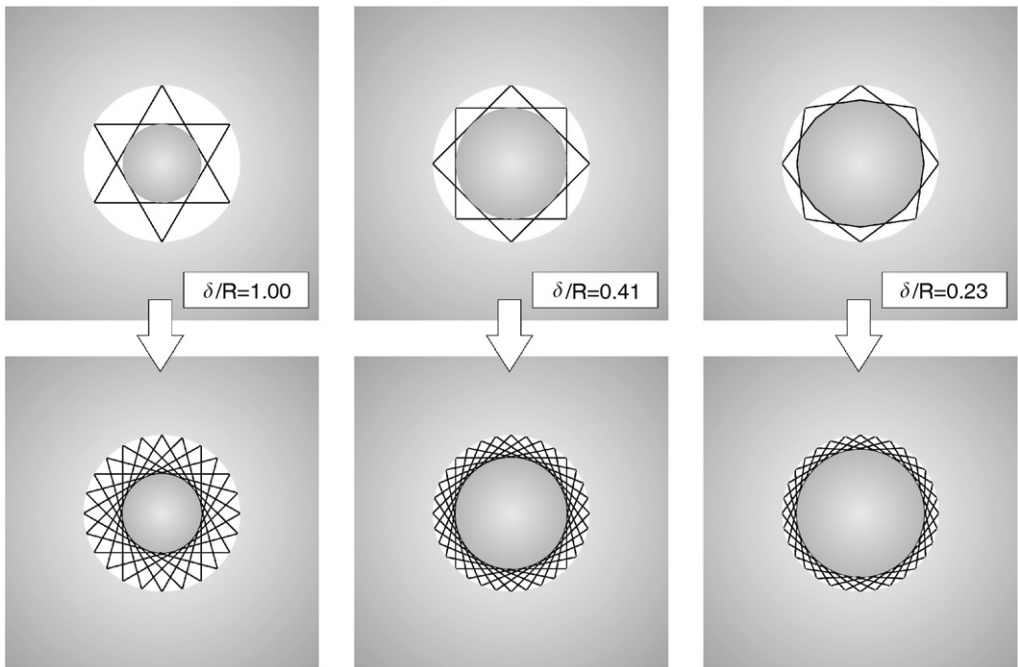


Fig. 5. Geometry of the interfacial structure permitting maximization of both the bulk and the shear moduli of the composite. Discrete (upper parts) and smeared (lower parts) structures.

First we note that, since from the conformal mapping

$$z = R \left( \zeta + \frac{m}{\zeta} \right), \quad (10)$$

we can obtain  $\zeta$  as

$$\zeta = \frac{z \pm \sqrt{z^2 - 4mR^2}}{2R} \quad (11)$$

and since we seek the leading-order (large  $r$ ) terms, we expand Eq. (11) in  $z/R$  and find for  $z/R$  large (note that only the + sign in Eq. (11) is physically correct)

$$\zeta = \rho e^{i\beta} = \frac{z}{R} + O\left(\frac{R}{z}\right) = \frac{r e^{i\theta}}{R} + O\left(\frac{R}{z}\right), \quad (12)$$

so that we conclude that a circle of radius  $r \gg R$  is mapped into a circle of radius  $\rho = r/R$  in the transformed domain such that  $\theta = \beta$ . Therefore, we can express the leading-order terms in the far field displacements as

$$\begin{aligned} u_r &= \frac{r}{8\mu} U_1(\theta) + \frac{R^2}{8\mu r} U_2(\theta) + \frac{R}{4\pi\mu r} U_3(\theta), \\ u_\theta &= \frac{r}{8\mu} U_4(\theta) + \frac{R^2}{4\mu r} U_5(\theta) + \frac{R}{4\pi\mu r} U_6(\theta), \end{aligned} \quad (13)$$

where

$$\begin{aligned} U_1(\theta) &= 4\sigma_{12}^\infty \sin 2\theta + \sum_{\alpha=1}^2 \sigma_{\alpha\alpha}^\infty [(\kappa - 1) + 2(3 - 2\alpha) \cos 2\theta], \\ U_2(\theta) &= 4(1 + \kappa + m \cos 2\theta) \sin 2\theta \sigma_{12}^\infty + \sum_{\alpha=1}^2 \sigma_{\alpha\alpha}^\infty [2(1 + m^2) - m(3 + \kappa) \cos 2\theta \\ &\quad + (3 - 2\alpha)(m(\cos 4\theta - 3) + 2 \cos 2\theta(1 + \kappa))], \\ U_3(\theta) &= - \sum_{k=1}^N \sum_{\alpha=1}^2 F_k^\alpha \left[ (1 + \kappa) \cos \left( 2\theta - \hat{\theta}_k^+ - \delta_{\alpha 2} \frac{\pi}{2} \right) + \cos \left( \hat{\theta}_k^- - \delta_{\alpha 2} \frac{\pi}{2} \right) \right. \\ &\quad \left. - m \cos \left( \hat{\theta}_k^+ + \delta_{\alpha 2} \frac{\pi}{2} \right) \right], \\ U_4(\theta) &= 2\sigma_{12}^\infty \cos 2\theta - \sum_{\alpha=1}^2 \sigma_{\alpha\alpha}^\infty (3 - 2\alpha) \sin 2\theta, \quad U_5(\theta) = [(\kappa - 1) + m \cos 2\theta] U_4(\theta), \\ U_6(\theta) &= \sum_{k=1}^N \sum_{\alpha=1}^2 F_k^\alpha \left[ (\kappa - 1) \sin \left( 2\theta - \hat{\theta}_k^+ - \delta_{\alpha 2} \frac{\pi}{2} \right) \right. \\ &\quad \left. + \sin \left( \hat{\theta}_k^- - \delta_{\alpha 2} \frac{\pi}{2} \right) - m \sin \left( \hat{\theta}_k^+ + \delta_{\alpha 2} \frac{\pi}{2} \right) \right], \end{aligned} \quad (14)$$

with  $\delta_{ij}$  denoting the Kronecker delta and  $F_k^\alpha = \{P_k, S_k\}$  and  $\hat{\theta}_k^+ = \beta_k + \theta_k^n$ ,  $\hat{\theta}_k^- = \beta_k - \theta_k^n$ , where  $\theta_k^n$  denotes the angle between the inward normal at the void boundary and the  $x_1$  (horizontal) axis at the node  $k$ .

From the far field displacement field, we obtain the leading-order terms in the far field stress

$$\begin{aligned}\sigma_{rr} &= S_1(\theta) + \frac{R^2}{2r^2} S_2(\theta) + \frac{R}{2\pi r^2} S_3(\theta), \\ \sigma_{r\theta} &= S_4(\theta) + \frac{R^2}{2r^2} S_5(\theta) + \frac{R}{2\pi r^2} S_6(\theta), \\ \sigma_{\theta\theta} &= S_7(\theta) + \frac{R^2}{2r^2} S_8(\theta) + \frac{R}{2\pi r^2} S_9(\theta),\end{aligned}\tag{15}$$

where

$$\begin{aligned}S_1(\theta) &= \sigma_{12}^\infty \sin 2\theta + \frac{1}{2} \sum_{\alpha=1}^2 \sigma_{\alpha\alpha}^\infty [1 + (3 - 2\alpha) \cos 2\theta], \\ S_2(\theta) &= 4(m \cos 2\theta - 2) \sin 2\theta \sigma_{12}^\infty + \sum_{\alpha=1}^2 \sigma_{\alpha\alpha}^\infty [4m \cos 2\theta - 1 - m^2 \\ &\quad + 2 \cos 2\theta (m \cos 2\theta - 2)(3 - 2\alpha)], \\ S_3(\theta) &= \sum_{k=1}^N \sum_{\alpha=1}^2 F_k^\alpha \left[ 4 \cos \left( 2\theta - \hat{\theta}_k^+ - \delta_{x2} \frac{\pi}{2} \right) + \cos \left( \hat{\theta}_k^- - \delta_{x2} \frac{\pi}{2} \right) \right. \\ &\quad \left. - m \cos \left( \hat{\theta}_k^+ + \delta_{x2} \frac{\pi}{2} \right) \right], \\ S_4(\theta) &= \sigma_{12}^\infty \cos 2\theta - \frac{1}{2} \sin 2\theta \sum_{\alpha=1}^2 \sigma_{\alpha\alpha}^\infty (3 - 2\alpha), \\ S_5(\theta) &= 4[\cos 2\theta - m \sin^2 2\theta] \sigma_{12}^\infty + 2 \sin 2\theta \sum_{\alpha=1}^2 \sigma_{\alpha\alpha}^\infty [m - (3 - 2\alpha)(1 + m \cos 2\theta)], \\ S_6(\theta) &= \sum_{k=1}^N \sum_{\alpha=1}^2 F_k^\alpha \left[ 2 \sin \left( 2\theta - \hat{\theta}_k^+ - \delta_{x2} \frac{\pi}{2} \right) - \sin \left( \hat{\theta}_k^- - \delta_{x2} \frac{\pi}{2} \right) \right. \\ &\quad \left. + m \sin \left( \hat{\theta}_k^+ + \delta_{x2} \frac{\pi}{2} \right) \right], \\ S_7(\theta) &= -\sigma_{12}^\infty \sin 2\theta + \frac{1}{2} \sum_{\alpha=1}^2 \sigma_{\alpha\alpha}^\infty [1 - (3 - 2\alpha) \cos 2\theta], \\ S_8(\theta) &= -2m \sigma_{12}^\infty \sin 4\theta + \sum_{\alpha=1}^2 \sigma_{\alpha\alpha}^\infty [1 + m^2 - m(3 - 2\alpha)(1 + \cos 4\theta)], \\ S_9(\theta) &= -\sum_{k=1}^N \sum_{\alpha=1}^2 F_k^\alpha \left[ \cos \left( \hat{\theta}_k^- - \delta_{x2} \frac{\pi}{2} \right) - m \cos \left( \hat{\theta}_k^+ + \delta_{x2} \frac{\pi}{2} \right) \right].\end{aligned}\tag{16}$$

Note that the resultant components  $P_k$  and  $S_k$  are functions of the geometry, the loading at infinity, and the elastic constants of the plane, elliptical inclusion and structural interface. In particular, compatibility at the elastic body/structure  $j$ th junction, where  $M$  bars converge, can be expressed as (see Eq. (9) in Part I of this paper, but now in terms of resultants, instead of quantities per unit length of the bar)

$$(P_k + iS_k)e^{i\theta_k^n} = \sum_{h=1}^M k_b^{(hk)} [(\mathbf{u}(\mathbf{x}_k) - \mathbf{u}(\mathbf{x}_h)) \cdot \mathbf{e}_{(hk)}^r] \mathbf{e}_{(hk)}^r, \quad (17)$$

where  $\mathbf{u}(\mathbf{x}_h)$  is the displacement at the  $h$ th junction central point  $\mathbf{x}_h$ ,  $k_b^{(hk)}$  is the stiffness of the  $hk$  bar, and  $\mathbf{e}_{(hk)}^r$  is the unit vector aligned parallel to the bar,

$$\mathbf{e}_{(hk)}^r = \frac{\mathbf{x}_k - \mathbf{x}_h}{|\mathbf{x}_k - \mathbf{x}_h|}. \quad (18)$$

Note that, with  $\mathbf{x}_h$  lying on the matrix,  $\mathbf{u}(\mathbf{x}_h)$  is due to both the remote stress applied ( $\mathbf{u}^\infty$ ) and the tractions applied at the junction ( $\mathbf{u}^{PS}$ )

$$\mathbf{u}(\mathbf{x}_h) = \mathbf{u}^\infty(\mathbf{x}_h) + \mathbf{u}^{PS}(\mathbf{x}_h); \quad (19)$$

otherwise, if  $\mathbf{x}_h$  lies on the inclusion,

$$\mathbf{u}(\mathbf{x}_h) = \mathbf{u}^{PS}(\mathbf{x}_h). \quad (20)$$

It is important now to note that  $\mathbf{u}^{PS}(\mathbf{x}_h)$  is a linear function of the load components  $P_k$  and  $S_k$ ,

$$\mathbf{u}^{PS}(\mathbf{x}_h) = \sum_{j=1}^N (V_{hj}P_j + W_{hj}S_j), \quad (21)$$

where the coefficients are determined by employing the complex potentials given in Eqs. (24) and (32) in Part I of this article for the elliptical inclusion and matrix, respectively. Note that the compatibility Eq. (17) needs to be written at each node of the interfacial structure, so that, after separation of its real and complex parts, a linear system of  $2N_{\text{tot}}$  equations is obtained

$$\mathbf{T}\{P_1, S_1, \dots, P_{N_{\text{tot}}}, S_{N_{\text{tot}}}\}^T = \mathbf{F}\{u_1^\infty(\mathbf{x}_1), u_2^\infty(\mathbf{x}_1), \dots, u_1^\infty(\mathbf{x}_N), u_2^\infty(\mathbf{x}_N)\}^T, \quad (22)$$

$N_{\text{tot}}$  denoting the total number of nodes of the structure. Therefore, the traction resultant components  $P_k$  and  $S_k$  at the  $k$ -junction can be solved for from Eq. (22) as

$$\begin{aligned} P_k &= \sum_{j=1}^N (\mathbf{T}^{-1}\mathbf{F})_{(2k-1)(2j-1)} u_1^\infty(\mathbf{x}_j) + (\mathbf{T}^{-1}\mathbf{F})_{(2k-1)2j} u_2^\infty(\mathbf{x}_j), \\ S_k &= \sum_{j=1}^N (\mathbf{T}^{-1}\mathbf{F})_{2k(2j-1)} u_1^\infty(\mathbf{x}_j) + (\mathbf{T}^{-1}\mathbf{F})_{2k2j} u_2^\infty(\mathbf{x}_j). \end{aligned} \quad (23)$$

Finally, to simplify the notation, we introduce the following matrices:

$$\begin{aligned} A_{jk} &= (\mathbf{T}^{-1}\mathbf{F})_{(2k-1)(2j-1)}, & B_{jk} &= (\mathbf{T}^{-1}\mathbf{F})_{(2k-1)2j}, \\ C_{jk} &= (\mathbf{T}^{-1}\mathbf{F})_{2k(2j-1)}, & D_{jk} &= (\mathbf{T}^{-1}\mathbf{F})_{2k2j}. \end{aligned} \quad (24)$$

We consider now a remote uniaxial stress  $\sigma_{11}^\infty$  and employ Eq. (23) in Eqs. (13) and (15), which, substituted in Eqs. (1), allows us to obtain the averaged stress and strain in the circular region of radius  $r$  containing an elliptical reinforced void or inclusion inclined at an angle  $\alpha$  with respect to the horizontal direction (truncated at first order in  $f$ )

$$\begin{aligned}\bar{\sigma}_{11} &= \sigma_{11}^\infty - f \sigma_{11}^\infty R^2 \frac{(2 + m^2 - 2m \cos 2\alpha)}{2ab} + \frac{f(1 + \kappa)R^2 \sigma_{11}^\infty}{16\pi ab\mu} \\ &\quad \times \sum_{j,k=1}^N [(\Gamma_j^0 A_{jk} + \Gamma_j^1 B_{jk})h_k^{(0,0,1)} + (\Gamma_j^0 C_{jk} + \Gamma_j^1 D_{jk})h_k^{(1,1,1)}], \\ \bar{\sigma}_{12} &= \frac{fmR^2 \sigma_{11}^\infty \sin 2\alpha}{2ab} + \frac{f(1 + \kappa)R^2 \sigma_{11}^\infty}{16\pi ab\mu} \sum_{j,k=1}^N [(\Gamma_j^0 A_{jk} + \Gamma_j^1 B_{jk}) \sin(\hat{\theta}_k^+ + 2\alpha) \\ &\quad + (\Gamma_j^0 C_{jk} + \Gamma_j^1 D_{jk}) \cos(\hat{\theta}_k^+ + 2\alpha)], \\ \bar{\sigma}_{22} &= -\frac{f\sigma_{11}^\infty m^2 R^2}{2ab} + \frac{f(1 + \kappa)R^2 \sigma_{11}^\infty}{16\pi ab\mu} \sum_{j,k=1}^N [(\Gamma_j^0 A_{jk} + \Gamma_j^1 B_{jk})h_k^{(0,2,1)} \\ &\quad + (\Gamma_j^0 C_{jk} + \Gamma_j^1 D_{jk})h_k^{(1,-1,1)}] \end{aligned} \quad (25)$$

and

$$\begin{aligned}\bar{\varepsilon}_{11} &= \sigma_{11}^\infty \frac{1 + \kappa}{8\mu} - fR^2 \sigma_{11}^\infty \frac{[m(9 + \kappa) \cos 2\alpha - 4(1 + \kappa + m^2)]}{16ab\mu} - \frac{f(1 + \kappa)R^2 \sigma_{11}^\infty}{32\pi ab\mu^2} \\ &\quad \times \sum_{j,k=1}^N [(\Gamma_j^0 A_{jk} + \Gamma_j^1 B_{jk})h_k^{(0,0,\kappa)} + (\Gamma_j^0 C_{jk} + \Gamma_j^1 D_{jk})h_k^{(1,1,\kappa)}], \\ \bar{\varepsilon}_{12} &= -\frac{fmR^2 \sigma_{11}^\infty (3 + \kappa) \sin 2\alpha}{16ab\mu} - \frac{f(1 + \kappa)R^2 \sigma_{11}^\infty}{32\pi ab\mu^2} \sum_{j,k=1}^N [(\Gamma_j^0 A_{jk} + \Gamma_j^1 B_{jk}) \sin(\hat{\theta}_k^+ + 2\alpha) \\ &\quad + (\Gamma_j^0 C_{jk} + \Gamma_j^1 D_{jk}) \cos(\hat{\theta}_k^+ + 2\alpha)], \\ \bar{\varepsilon}_{22} &= \sigma_{11}^\infty \frac{\kappa - 3}{8\mu} - f\sigma_{11}^\infty R^2 \frac{4(1 - \kappa + m^2) + (\kappa - 3)m \cos 2\alpha}{16ab\mu} - \frac{f(1 + \kappa)R^2 \sigma_{11}^\infty}{32\pi ab\mu^2} \\ &\quad \times \sum_{j,k=1}^N [(\Gamma_j^0 A_{jk} + \Gamma_j^1 B_{jk})h_k^{(0,-2,\kappa)} + (\Gamma_j^0 C_{jk} + \Gamma_j^1 D_{jk})h_k^{(1,-1,\kappa)}], \end{aligned} \quad (26)$$

where  $f = ab/r^2$  and

$$\begin{aligned}\Gamma_j^p &= [1 - (-1)^p m] \cos\left(\beta_j - p\frac{\pi}{2}\right) + 2 \cos\left(\beta_j + 2\alpha + p\frac{\pi}{2}\right), \\ h_k^{(p,q,\kappa)} &= \cos\left(\hat{\theta}_k^- - p\frac{\pi}{2}\right) - m \cos\left(\hat{\theta}_k^+ + p\frac{\pi}{2}\right) + q \cos\left(\hat{\theta}_k^+ + 2\alpha + q\frac{\pi}{2}\right). \end{aligned} \quad (27)$$

In order to analyze a dilute suspension of randomly oriented elliptical inclusions, an isotropic average, defined for an arbitrary function  $g$  of angle  $\alpha$  as

$$g^{is} = \frac{1}{2\pi} \int_0^{2\pi} g(\alpha) d\alpha, \quad (28)$$

is employed, yielding

$$\begin{aligned} \bar{\sigma}_{11}^{is} &= \sigma_{11}^{\infty} - f\sigma_{11}^{\infty}R^2 \frac{2+m^2}{2ab} + \frac{f(1+\kappa)R^2\sigma_{11}^{\infty}}{16ab\pi\mu} \sum_{j,k=1}^N [A_{jk}(v_{jk}^{(0,0,0)} + w_{jk}^{(1,1,1)}) \\ &\quad + B_{jk}(v_{jk}^{(1,1,0)} - w_{jk}^{(1,0,1)}) + C_{jk}(v_{jk}^{(0,0,1)} + w_{jk}^{(1,0,1)}) + D_{jk}(v_{jk}^{(1,1,1)} + w_{jk}^{(1,1,1)})], \\ \bar{\sigma}_{12}^{is} &= \frac{f(1+\kappa)R^2\sigma_{11}^{\infty}}{16ab\pi\mu} \sum_{j,k=1}^N [(C_{jk} - B_{jk})\cos(\beta_j - \hat{\theta}_k^+) - (A_{jk} + D_{jk})\sin(\beta_j - \hat{\theta}_k^+)], \\ \bar{\sigma}_{22}^{is} &= -\frac{f\sigma_{11}^{\infty}m^2R^2}{2ab} + \frac{f(1+\kappa)R^2\sigma_{11}^{\infty}}{16ab\pi\mu} \sum_{j,k=1}^N [A_{jk}(v_{jk}^{(0,0,0)} - w_{jk}^{(1,1,1)}) \\ &\quad + B_{jk}(v_{jk}^{(1,1,0)} + w_{jk}^{(1,0,1)}) + C_{jk}(v_{jk}^{(0,0,1)} - w_{jk}^{(1,0,1)}) + D_{jk}(v_{jk}^{(1,1,1)} - w_{jk}^{(1,1,1)})], \end{aligned} \quad (29)$$

and

$$\begin{aligned} \bar{\varepsilon}_{11}^{is} &= \sigma_{11}^{\infty} \frac{1+\kappa}{8\mu} + f\sigma_{11}^{\infty}R^2 \frac{1+\kappa+m^2}{4ab\mu} - \frac{f(1+\kappa)R^2\sigma_{11}^{\infty}}{32ab\pi\mu^2} \sum_{j,k=1}^N [A_{jk}(v_{jk}^{(0,0,0)} + w_{jk}^{(k,0,0)}) \\ &\quad + B_{jk}(v_{jk}^{(1,1,0)} + w_{jk}^{(k,1,0)}) + C_{jk}(v_{jk}^{(0,0,1)} - w_{jk}^{(k,1,0)}) + D_{jk}(v_{jk}^{(1,1,1)} + w_{jk}^{(k,0,0)})], \\ \bar{\varepsilon}_{12}^{is} &= -\frac{\kappa}{2\mu} \bar{\sigma}_{12}^{is}, \\ \bar{\varepsilon}_{22}^{is} &= \sigma_{11}^{\infty} \frac{\kappa-3}{8\mu} + f\sigma_{11}^{\infty}R^2 \frac{1-\kappa+m^2}{4ab\mu} - \frac{f(1+\kappa)R^2\sigma_{11}^{\infty}}{32ab\pi\mu^2} \sum_{j,k=1}^N [A_{jk}(v_{jk}^{(0,0,0)} - w_{jk}^{(k,0,0)}) \\ &\quad + B_{jk}(v_{jk}^{(1,1,0)} - w_{jk}^{(k,1,0)}) + C_{jk}(v_{jk}^{(0,0,1)} + w_{jk}^{(k,1,0)}) + D_{jk}(v_{jk}^{(1,1,1)} - w_{jk}^{(k,0,0)})], \end{aligned} \quad (30)$$

where

$$\begin{aligned} v_{jk}^{(p,g,q)} &= [(-1)^p - m] \cos\left(\beta_j + g\frac{\pi}{2}\right) \left[ (-1)^q \cos\left(\hat{\theta}_k^- + q\frac{\pi}{2}\right) - m \cos\left(\hat{\theta}_k^+ + q\frac{\pi}{2}\right) \right], \\ w_{jk}^{(p,g,q)} &= p \cos\left(\beta_j - \hat{\theta}_k^+ + g\frac{\pi}{2} - q\frac{\pi}{2}\right). \end{aligned} \quad (31)$$

We note that we have always found  $\bar{\sigma}_{12}^{is} = \bar{\varepsilon}_{12}^{is} = 0$ , a result consistent with the symmetry enforced by the isotropic averaging (28).

We are now in a position to determine the effective moduli for the composite; employing Eqs. (2), we obtain (considering only up through linear terms in  $f$ )

$$\begin{aligned} \frac{\bar{\mu}}{\mu} &= 1 + \frac{f(a+b)^2(1+\kappa)}{32ab\pi\mu} \left\{ -8\mu\pi + (1+\kappa) \sum_{j,k=1}^N [(A_{jk} + D_{jk}) \cos(\beta_j - \hat{\theta}_k^+) \right. \\ &\quad \left. - (B_{jk} - C_{jk}) \sin(\beta_j - \hat{\theta}_k^+)] \right\}, \\ \frac{\bar{K}}{K} &= 1 + \frac{f(1+\kappa)}{8\mu ab\pi(\kappa-1)} \left\{ -4(a^2 + b^2)\mu\pi + (\kappa+1) \sum_{j,k=1}^N [A_{jk}(b^2 g_{jk}^{(0,0,0)} + abg_{jk}^{(0,1,1)}) \right. \\ &\quad - B_{jk}(abg_{jk}^{(1,0,0)} + a^2 g_{jk}^{(1,1,1)}) - C_{jk}(abg_{jk}^{(0,1,0)} - b^2 g_{jk}^{(0,0,1)}) \\ &\quad \left. + D_{jk}(a^2 g_{jk}^{(1,1,0)} - abg_{jk}^{(1,0,1)})] \right\}, \end{aligned} \quad (32)$$

where

$$g_{jk}^{(p,q,q)} = \cos\left(\beta_j + q\frac{\pi}{2}\right) \cos\left(\beta_k + g\frac{\pi}{2}\right) \cos\left(\theta_k^n + q\frac{\pi}{2}\right). \quad (33)$$

We note that the effective moduli given by Eq. (32), in the limit case of a void (i.e. in the absence of a structural interface), reduce to

$$\frac{\bar{\mu}}{\mu} = 1 - f(1+\kappa) \frac{(a+b)^2}{4ab}, \quad \frac{\bar{K}}{K} = 1 - f \frac{1+\kappa}{\kappa-1} \frac{a^2 + b^2}{2ab}, \quad (34)$$

which coincide with those reported by Jasiuk et al. (1994) for a dilute composite with randomly oriented elliptical holes.

As an application of the expressions for the effective properties (32), the effective shear and bulk moduli for an infinite elastic plane with a dilute suspension of randomly oriented cracks of length  $2a$  reinforced with two fibers orthogonal to the fracture surface (having locations  $x$  and  $-x$  from the central point of the crack) is considered (see the detail in Fig. 6, right). In this case,  $S_k = 0$  and only  $u_2^\infty$  contributes to the fiber elongation, so that  $A_{jk} = C_{jk} = D_{jk} = 0$ . For a crack density  $n$ , the volume concentration  $f$  is given by  $f = n\pi ab$ , so that, taking the limit for  $b \rightarrow 0$ , Eqs. (32) reduce to

$$\begin{aligned} \frac{\bar{\mu}}{\mu} &= 1 - \frac{(1+\kappa)a^2 n}{4} \left( \pi + \frac{1+\kappa}{8\mu} \sum_{j,k=1}^4 B_{jk} \sin(\beta_j - \hat{\theta}_k^+) \right), \\ \frac{\bar{K}}{K} &= 1 - \frac{(1+\kappa)a^2 n}{2(\kappa-1)} \left( \pi - \frac{1+\kappa}{4\mu} \sum_{j,k=1}^4 B_{jk} \sin\beta_j \sin\beta_k \sin\theta_k^n \right), \end{aligned} \quad (35)$$

where, numbering the junctions as in the detail of Fig. 6 (right),  $B_{jk}$  are

$$\begin{aligned} B_{11} &= -B_{41} = B_{22} = -B_{32} = Vt_b [aA^{(2)}k(1+\kappa) - 8\pi\mu], \\ B_{21} &= -B_{31} = B_{12} = -B_{42} = -VaA^{(1)}kt_b(1+\kappa), \\ B_{j3} &= B_{j2}, \quad B_{j4} = B_{j1}, \end{aligned} \quad (36)$$

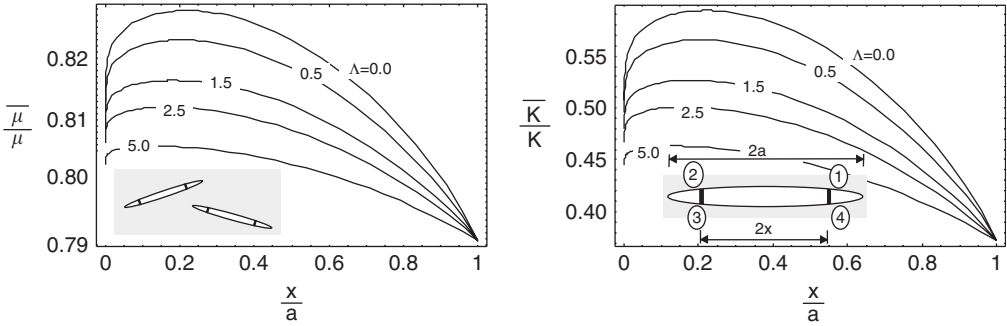


Fig. 6. Effective shear modulus  $\bar{\mu}$  (left) and 2D bulk modulus  $\bar{K}$  (right) (normalized by  $\mu$  and  $K$ , respectively) for a dilute suspension of randomly oriented sharp cracks of length  $2a$  reinforced by two symmetrical transverse fibers located at  $x$  and  $-x$ , for different values of the fibers compliance parameter  $\Lambda$ .

in which

$$V = \frac{8k\pi\mu}{a^2k^2(1 + \kappa)^2[(A^{(1)})^2 - (A^{(2)})^2] + 16aA^{(2)}k(1 + \kappa)\pi\mu - 64\pi^2\mu^2},$$

$$A^{(h)} = - \sum_{\alpha=1}^2 (-1)^\alpha \left[ 4\beta_\alpha \sin \beta + 2(\cos \beta - (-1)^h \cos \beta_\alpha) \log \left| \frac{-1 + (-1)^h \cos(\beta_\alpha + \beta)}{-1 + (-1)^h \cos(\beta_\alpha - \beta)} \right| \right], \tag{37}$$

with  $\beta_1 = \beta^-$  and  $\beta_2 = \beta^+$ .

Note that in the absence of fibers,  $B_{11} = B_{21} = 0$ , Eqs. (35) reduce to the well-known formulae for a dilute suspension of randomly oriented cracks (Kachanov et al., 1994).

The variation of averaged shear modulus  $\bar{\mu}$  and 2D bulk modulus  $\bar{K}$  (normalized by  $\mu$  and  $K$ , respectively) as a function of the fiber position is shown in Fig. 6, for  $t_b/a = \frac{1}{1000}$ , crack density  $n = 0.001$ , and different values of the dimensionless compliance parameter  $\Lambda = 2\mu^+ / [(\kappa^+ + 1)kt_b]$  (see Eq. (35) of Part I). First we note that as  $\Lambda$  increases, the averaged moduli tend to those corresponding to an unreinforced crack,  $\bar{\mu}/\mu = 0.79$  and  $\bar{K}/K = 0.37$ . The effect of the fibers vanishes when they are close to the crack tip, whereas it is maximum for  $x/a \simeq 0.2$ . We conclude that fibers close to the crack tip drastically reduce the stress singularity, but are almost ineffective for enhancing the overall elastic properties.

As a final example, the effective shear and bulk moduli for an infinite elastic plane with a dilute suspension of randomly oriented elliptical (thin,  $a/b = 20$ ) voids reinforced by rigid fibers ( $\Lambda = 0$ ) is plotted in Fig. 7, for an inclusion volume fraction  $f = 0.005$ . The results model the averaged stiffness coefficients of a cracked fiber-reinforced material, such as that reported in Fig. 1(B) of Part I of this article, a situation not previously investigated.

The fibers are characterized by  $t_b/a = \frac{1}{1000}$  and two different distributions are considered: purely orthogonal to the major axis (marked in Fig. 7 as ‘vertical’) and randomly distributed and oriented (marked as ‘random’ in Fig. 7). The averaged properties for a dilute suspension of randomly oriented rigid inclusions are given by the well-known

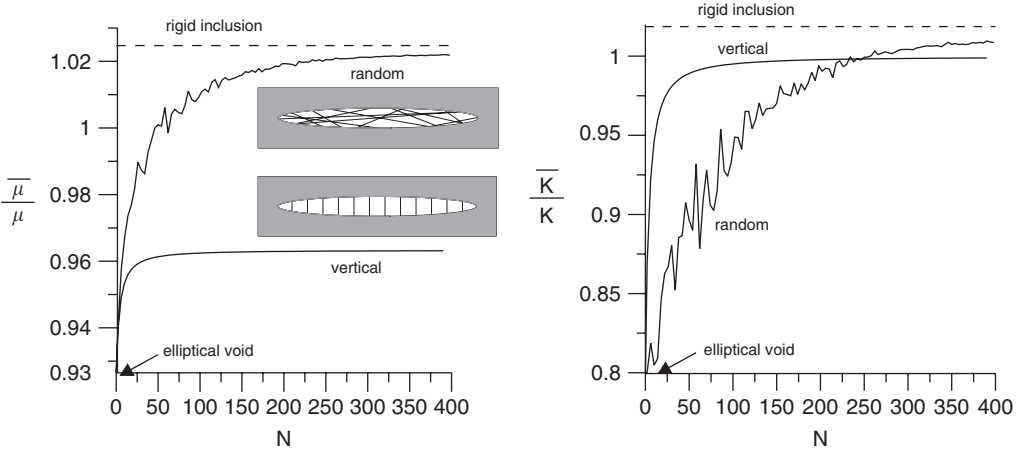


Fig. 7. Effective shear modulus  $\bar{\mu}$  (left) and 2D bulk modulus  $\bar{K}$  (right) (normalized by  $\mu$  and  $K$ , respectively) for a dilute distribution ( $f = 0.005$ ) of randomly oriented elliptical voids ( $a/b = 20$ ), reinforced by  $N$  rigid fibers ( $A = 0$ ). Two different fiber distributions are considered: purely vertical and randomly oriented and distributed.

formulae

$$\frac{\bar{\mu}}{\mu^+} = 1 + f \frac{m^2 + \kappa^+[2 - \kappa^+(m^2 - 2)]}{2\kappa^+(1 - m^2)(\kappa^+ + m^2)}, \quad \frac{\bar{K}}{K^+} = 1 + f \frac{(\kappa^+ - m^2)(1 + \kappa^+)}{2\kappa^+(1 - m^2)}, \quad (38)$$

as reported by Thorpe and Sen (1985), so that for an inclusion characterized by  $a/b = 20$ ,  $\bar{\mu}/\mu = 1.024$  and  $\bar{K}/K = 1.019$ . These values are *not* approached in the case of (highly dense) parallel vertical fibers, since in this case the reinforcement remains weak in the direction perpendicular to the fibers, but those values are approached in the case of randomly distributed fibers. Note that the oscillations in the graph are due to the fact that only one random distribution of fibers is considered for each  $N$ .

### 2.2.1. Circular inclusions coated by a discrete structural interface: effective properties

In the particular case of a circular inclusion of radius  $R$  connected to an infinite matrix having a circular hole of radius  $R + \delta$  by a discrete structural interface, Eqs. (32) simplify to

$$\frac{\bar{\mu}}{\mu} = 1 - f(1 + \kappa) \left\{ 1 - \frac{1 + \kappa}{8\pi\mu} \sum_{j,k=1}^N [(A_{jk} + D_{jk}) \cos(\beta_j - 2\theta_k) - (B_{jk} - C_{jk}) \sin(\beta_j - 2\theta_k)] \right\}, \quad (39)$$

$$\frac{\bar{K}}{K} = 1 + \frac{f(1 + \kappa)}{\kappa - 1} \left[ -1 + \frac{1 + \kappa}{8\mu\pi} \sum_{j,k=1}^N (A_{jk} \cos \beta_j + B_{jk} \sin \beta_j) \right].$$

As an example, the effective shear modulus  $\bar{\mu}$  and bulk modulus  $\bar{K}$  (normalized by  $\mu^+$  and  $K^+$ , respectively) are determined for a dilute suspension ( $f = 0.1$ ) of circular inclusions coated by a discrete structural interface with thickness  $\delta = R$ . Two different interfacial

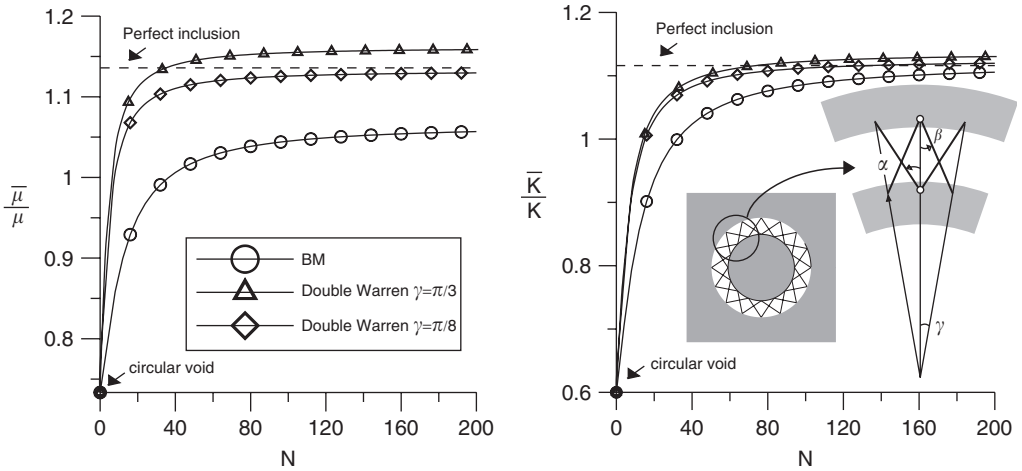


Fig. 8. Effective shear modulus  $\bar{\mu}$  (left) and 2D bulk modulus  $\bar{K}$  (right) (normalized by  $\mu$  and  $K$ , respectively) for a dilute distribution ( $f = 0.1$ ) of circular inclusions of radius  $R$  connected to an infinite matrix having a circular hole of radius  $R + \delta$  ( $\delta/R = 1$ ) by a double Warren truss structure comprised of  $4N$  rigid fibers ( $A = 0$ ). The matrix is stiffer than the inclusions ( $\mu^-/\mu^+ = 0.1$ ) and  $\nu^+ = \nu^- = \frac{1}{3}$ .

structures are considered: the discrete BM-model (from Bigoni and Movchan (2002), see Part I of this article) and a double Warren truss structure with two different opening angles  $\gamma = \{\pi/3, \pi/8\}$  (see detail in Fig. 8), corresponding to  $\alpha \simeq \{\pi/2, \pi/4\}$ . The elastic materials are characterized by  $\mu^-/\mu^+ = 10$  and  $\nu^- = \nu^+ = \frac{1}{3}$ , while the bars of thickness  $t_b/R = \frac{1}{1000}$  are assumed to be rigid ( $A = 0$ ). The effective moduli are reported in Fig. 8 at increasing bar density  $N$  ( $4N$  for the double Warren structure). It is clear from the figure that the non-locality introduced by the bars' inclination increases the averaged properties of the composite.

In the particular case of a dilute suspension of circular holes, the averaged properties are equal to  $\bar{\mu}/\mu^+ = 0.733$  and  $\bar{K}/K^+ = 0.6$ , the values approached in the graphs when the numbers of bars approaches zero. On the other hand, for a dilute suspension of circular inclusions connected to the matrix by a perfect interface, the averaged properties are equal to  $\bar{\mu}/\mu^+ = 1.14$  and  $\bar{K}/K^+ = 1.12$ , values approached in the graphs as the number of bars increases. In closure, we note that a dilute suspension of circular inclusions coated by a sufficiently dense structural interface is characterized by averaged properties higher than those corresponding to the perfect interface and that, increasing the bar density, the averaged properties tend to those predicted by the continuous model.

**3. Optimal stress distribution: neutrality**

The possibility of tuning the properties of the interface, so that an ‘optimal’ stress distribution is achieved, is investigated in this section. Optimality is intended here to correspond to a minimum stress concentration near the interface in the matrix, a condition which is fully satisfied when the inclusion is neutral. Previously, Ru (1998) analyzed the design of neutral elastic inclusions employing the zero-thickness linear interface, while Bigoni et al. (1998) investigated for the same structure a weaker condition of neutrality.

We show here that by employing a continuous structural interface, neutrality occurs for a range of material parameters broader than for a zero-thickness linear interface. A new concept of weak neutrality (coincident with the notions of neutrality employed by [Ru, 1998](#) and [Bigoni et al., 1998](#) only in particular cases) is introduced for inclusions coated by discrete structural interfaces, and it is shown that for a weakly neutral inclusion the perturbation introduced in the matrix is very localized, although non-null at every point of the matrix, as the notion of strong neutrality implies.

*3.1. Strong- and weak-neutrality conditions for an inclusion connected to the matrix by a structural interface*

Let us consider a generic inclusion connected to an elastic matrix by a structural interface, as shown in [Fig. 9](#), and subject to a remote uniform stress  $\sigma^\infty$ . Denoting by a superscript  $p$  the perturbation induced by the inclusion, we have

$$\mathbf{u} = \mathbf{u}^p + \mathbf{u}^\infty, \quad \boldsymbol{\varepsilon} = \boldsymbol{\varepsilon}^p + \boldsymbol{\varepsilon}^\infty, \quad \boldsymbol{\sigma} = \boldsymbol{\sigma}^p + \boldsymbol{\sigma}^\infty. \tag{40}$$

The strain energy in the elastic matrix contained within a contour  $\Gamma$  enclosing the inclusion,  $W_m$ , can be expressed as

$$W_m = \frac{1}{2} \int_{V^+} (\boldsymbol{\sigma}^\infty \cdot \boldsymbol{\varepsilon}^\infty + \boldsymbol{\sigma}^p \cdot \boldsymbol{\varepsilon}^p + \boldsymbol{\sigma}^\infty \cdot \boldsymbol{\varepsilon}^p + \boldsymbol{\sigma}^p \cdot \boldsymbol{\varepsilon}^\infty), \tag{41}$$

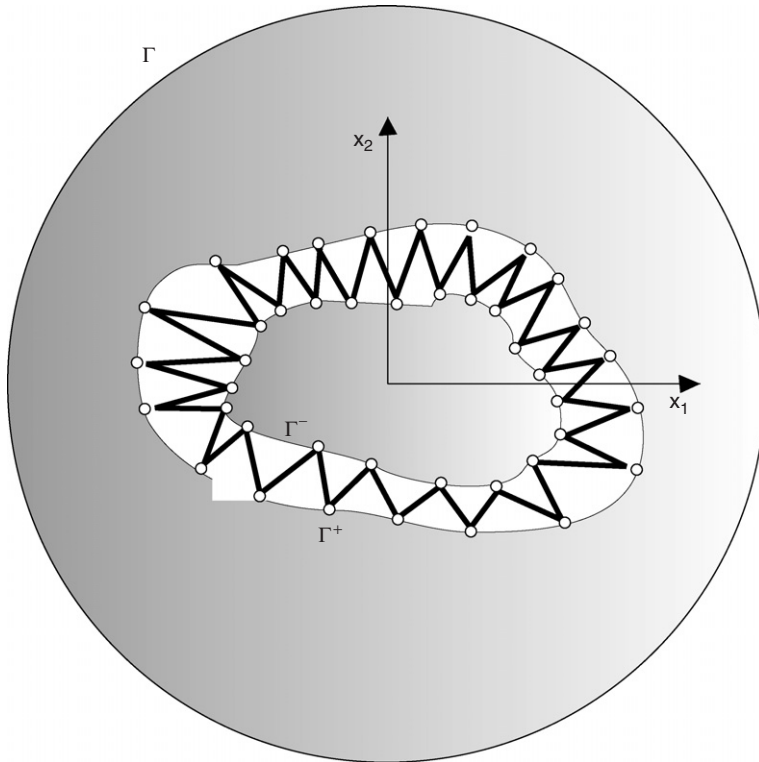


Fig. 9. Elastic inclusion and structural interface.

where  $V^+$  is the volume enclosed between  $\Gamma$  and the contour  $\Gamma^+$ , defining the boundary of the structural interface. On application of the divergence theorem, Eq. (41) becomes

$$W_m = \frac{1}{2} \int_{\tilde{\Gamma}} (\mathbf{t}^\infty \cdot \mathbf{u}^\infty + \mathbf{t}^p \cdot \mathbf{u}^p + \mathbf{t}^\infty \cdot \mathbf{u}^p + \mathbf{t}^p \cdot \mathbf{u}^\infty), \quad (42)$$

where  $\mathbf{t} = \boldsymbol{\sigma} \mathbf{n}$  denotes the traction vector and

$$\int_{\tilde{\Gamma}} = \int_{\Gamma} - \sum_{h=1}^{N^+} \int_{\omega_h^+}, \quad (43)$$

where  $N^+$  is the number of the junction regions  $\omega_h^+$  lying on  $\Gamma^+$  (see Part I, Section 2). The last term on the right-hand side of Eq. (43) is equal to the strain energy  $W_i$  in the structural interface and inclusion (changed in sign).

Therefore, the strain energy in the region enclosed by the contour  $\Gamma$  is the sum of the contributions of the matrix, structural interface and inclusion, viz.

$$W = W_m + W_i = \frac{1}{2} \int_{\Gamma} (\mathbf{t}^\infty \cdot \mathbf{u}^\infty + \mathbf{t}^p \cdot \mathbf{u}^p + \mathbf{t}^\infty \cdot \mathbf{u}^p + \mathbf{t}^p \cdot \mathbf{u}^\infty), \quad (44)$$

and it can be observed that  $W$  diverges as  $b \rightarrow \infty$ . However, this divergence is due to the fact that the unperturbed solution corresponds to a homogeneously stressed infinite domain, so that its energy is necessarily infinite. Therefore, the quantity

$$W - \frac{1}{2} \int_{\Gamma} \mathbf{t}^\infty \cdot \mathbf{u}^\infty = \frac{1}{2} \int_{\Gamma} (\mathbf{t}^p \cdot \mathbf{u}^p + \mathbf{t}^\infty \cdot \mathbf{u}^p + \mathbf{t}^p \cdot \mathbf{u}^\infty) \quad (45)$$

remains finite. This is zero in the absence of any inclusion and can be viewed as the perturbation of the energy due to the presence of the inclusion. Therefore, we take as a definition of strong inclusion neutrality the condition that the energy perturbation (45) be zero for all the ‘control’ volumes singled out by contour  $\Gamma$ , namely

$$\int_{\Gamma} (\mathbf{t}^p \cdot \mathbf{u}^p + \mathbf{t}^\infty \cdot \mathbf{u}^p + \mathbf{t}^p \cdot \mathbf{u}^\infty) = 0, \quad \forall \Gamma. \quad (46)$$

This definition of neutrality is equivalent to that employed by Milton and Serkov (2001) and Ru (1998).

The problem with applying (46) to discrete structural interfaces is that the matrix will be always ‘overstressed’ at the bar junctions, where a strong-neutrality condition will in general be violated. We prefer therefore to introduce a new, weak notion of neutrality. In particular, specializing  $\Gamma$  to a circle of radius  $d$  and taking the limit for  $d \rightarrow \infty$  of Eq. (46) we obtain

$$\lim_{d \rightarrow \infty} \int_{\Gamma(d)} \mathbf{t}^p \cdot \mathbf{u}^p \rightarrow 0, \quad (47)$$

so that

*we take as a definition of inclusion ‘weak neutrality’ the condition that the energy perturbation (45) be zero for  $d \rightarrow \infty$ , namely*

$$\lim_{d \rightarrow \infty} \int_{\Gamma(d)} (\mathbf{t}^\infty \cdot \mathbf{u}^p + \mathbf{t}^p \cdot \mathbf{u}^\infty) = 0. \quad (48)$$

That condition (48) is connected to neutrality is obvious since it is a weak form of (46). However, it is proven below that for a continuous structural interface (thus including as particular cases perfect and zero-thickness linear interfaces), connecting a *circular* inclusion to a matrix, condition (48) is equivalent to requiring the material's effective properties to be equal to the properties of the matrix material ( $\bar{\mu}/\mu = \bar{K}/K = 1$ ) for a dilute suspension of inclusions, a condition of neutrality also employed by Bigoni et al. (1998).

### 3.2. Strong- and weak-neutrality for a circular inclusion connected to an infinite matrix by a continuous structural interface

We start by considering a circular inclusion of radius  $R$  connected to an infinite matrix having a circular hole of radius  $R + \delta$  by a continuous double Warren truss structure (see Fig. 1). Since when a uniform stress is applied at infinity, the stress and displacement fields are derived from Eqs. (49) of Part I of this article, choosing  $\Gamma$  as a circle of radius  $d$  centered at the inclusion center, Eq. (46) can be rewritten in matrix form as

$$\boldsymbol{\sigma}^\infty \cdot \mathbf{H}\boldsymbol{\sigma}^\infty = 0, \quad \iff \quad \det \mathbf{H} = 0, \quad (49)$$

where

$$\boldsymbol{\sigma}^\infty = [\sigma_{11}^\infty, \sigma_{12}^\infty, \sigma_{22}^\infty]^T, \quad (50)$$

and the coefficients of the symmetric matrix  $\mathbf{H}$  are

$$\begin{aligned} H_{11} &= H_{33} = \frac{F_m \pi}{4d^2 \mu^+} [d^2(\kappa^+ - 3) - 4F_m] + \frac{1}{4} H_{22}, \\ H_{22} &= -\frac{2\pi}{d^6 \mu^+} \{6M_m^2 - 12B_m M_m d^2 + B_m d^4 [d^2(1 - \kappa^+) + 2B_m(\kappa^+ + 3)]\}, \\ H_{13} &= H_{11} - \frac{1}{2} H_{22}, \quad H_{12} = H_{23} = 0, \end{aligned} \quad (51)$$

in which  $B_m$ ,  $F_m$  and  $M_m$  are given by Eqs. (51) in Part I of this article. The form of the neutrality condition given in Eq. (49) is instructive, since it reveals that *if the eigenvalues of  $\mathbf{H}$  are distinct, neutrality holds only for certain loading at infinity*, corresponding to the eigenvector related to the vanishing eigenvalue.

We are now in a position to compute the eigenvalues  $h_i$  and the corresponding eigenvectors  $\mathbf{v}_i$  of the matrix  $\mathbf{H}$ , which turn out to be

$$\begin{aligned} h_1 &= \frac{\pi F_m}{2d^2 \mu^+} [d^2(\kappa^+ - 3) - 4F_m], \\ h_2 = h_3 &= -\frac{2\pi}{d^6 \mu^+} \{6M_m^2 - 12B_m M_m d^2 + B_m d^4 [2B_m(\kappa^+ + 3) + (1 - \kappa^+)d^2]\}, \\ \mathbf{v}_1 &= [1, 0, 1]^T, \quad \mathbf{v}_2 = \mathbf{v}_3 = [0, 1, 0]^T, \end{aligned} \quad (52)$$

showing that an inclusion can be neutral for equibiaxial stress or pure shear. The condition of strong neutrality requires vanishing of  $h_1$  or  $h_2$  for every  $d$ , whereas weak neutrality corresponds to the vanishing of  $h_1$  or  $h_2$ , but computed at the limit  $d \rightarrow \infty$ , so that

*Strong neutrality :*

$$\begin{aligned} F_m &= 0 && \text{for equibiaxial tension;} \\ B_m = M_m &= 0 && \text{for shear.} \end{aligned} \quad (53)$$

*Weak neutrality :*

$$\begin{aligned} F_m &= 0 && \text{for equibiaxial tension;} \\ B_m &= 0 && \text{for shear.} \end{aligned}$$

Therefore, there is no difference between strong and weak neutrality for equibiaxial remote stress, whereas the difference is in the requirement of  $M_m$  vanishing for remote shear. Note that in the case of weak neutrality, for an infinite matrix characterized by  $\kappa = 3$  ( $\kappa = 1$ ), the eigenvalue  $h_1$  ( $h_3$ ) is identically zero; for these cases higher-order terms should be considered in the energy.

For a dilute suspension of circular inclusions connected to an infinite matrix by a continuous double Warren truss structure, the averaged properties are given by Eq. (5), so that it is clear from Eq. (53) that the condition of weak neutrality under equibiaxial tension is equivalent to  $\bar{K}/K^+ = 1$ , whereas the condition of weak neutrality under shear is equivalent to  $\bar{\mu}/\mu^+ = 1$ .<sup>3</sup>

The following can be concluded from the conditions of strong and weak neutrality:

- It is possible to choose the interfacial properties to satisfy weak neutrality (coincident for circular inclusions with  $\bar{K}/K^+ = \bar{\mu}/\mu^+ = 1$ ) for *both* remote equibiaxial stress and pure shear (i.e.  $F_m = B_m = 0$ , or, in other words,  $h_1 = h_2 = 0$ ). A circular inclusion connected to the matrix by a zero-thickness linear interface is weakly neutral for both remote shear and equibiaxial tension when the conditions found by Bigoni et al. (1998, their Eqs. (43)–(44)) are met, which is possible only for inclusions stiffer than the matrix. For a circular inclusion coated by a continuous structural interface, the solution of the conditions  $B_m = F_m = 0$  in the plane  $\mu^-/\mu^+$  versus  $\delta/R$  is reported in Fig. 10, for  $\nu^+ = \nu^- = \frac{1}{3}$  and different bar inclinations  $\alpha$ . It is clear that employing a continuous structural interface, weak neutrality becomes possible also for  $\mu^-/\mu^+ < 1$ .
- In the case of strong neutrality, the stress at each point of the matrix is the same as in the absence of the inclusion. However, as in the case of the zero-thickness linear interface (Ru, 1998), *differently from weak neutrality*, it is not possible to choose the interfacial properties to satisfy strong neutrality for *both* remote equibiaxial stress and pure shear (i.e.  $F_m = B_m = M_m = 0$ );
- For remote equibiaxial traction, strong neutrality occurs when  $F_m = 0$  (see Eq. (53)), which in terms of bar stiffness  $k$  becomes

$$k = \frac{2\mu^- \mu^+ (R + \delta)}{(1 - \kappa^-)R(R + \delta)\mu^+ \cos^2 \alpha + (\kappa^+ - 1)\mu^- (R^2 \cos^2 \alpha + 2R\delta + \delta^2)}. \quad (54)$$

<sup>3</sup>The coincidence between weak neutrality and the criterion  $\bar{K}/K^+ = \bar{\mu}/\mu^+ = 1$  (for circular inclusions) is valid also as particular cases for a zero-thickness interface (in this case the coefficients  $B_m$  and  $F_m$  are given by Eqs. (54) in Part I of this article) and for a perfectly bonded interface.

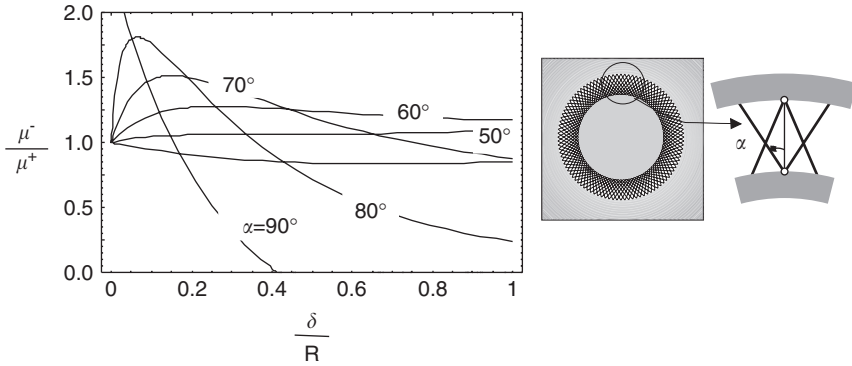


Fig. 10. Circular inclusion of radius  $R$  connected to an infinite matrix by a continuous double Warren truss structure of thickness  $\delta$  and bars inclination  $\alpha$ . Combinations of parameters  $\mu^-/\mu^+$  and  $\delta/R$  for which weak neutrality is possible under both remote equibiaxial tension and shear ( $F_m = B_m = 0$ ). Different bar inclinations  $\alpha$  are considered.

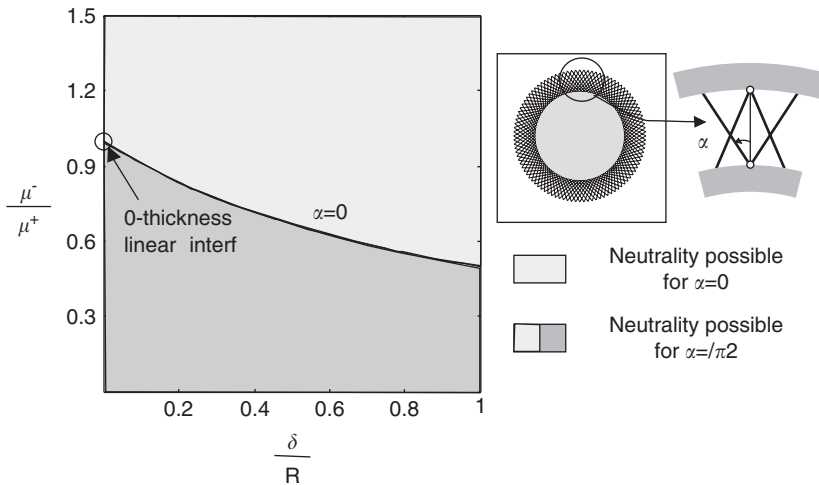


Fig. 11. Circular inclusion of radius  $R$  connected to an infinite matrix by a continuous double Warren truss structure of thickness  $\delta$  and bar inclinations  $\alpha = \{0, \pi/2\}$ . Range of parameters  $\mu^-/\mu^+$ , and  $\delta/R$  for which inclusion strong neutrality becomes possible under remote equibiaxial stress. Admissibility corresponds to all points in both the gray zones for  $\alpha = \pi/2$  and in the light gray zone for  $\alpha = 0$ .

In the limit case of a linear zero-thickness interface [ $\delta \rightarrow 0$  and  $\alpha \rightarrow \arctan(cR)$ , see Eq. (46) in Part I of this paper], Eq. (54) reduces to a condition found by Ru (1998)

$$k_r = \frac{4\mu^- \mu^+}{R[(\kappa^+ - 1)\mu^- - \mu^+(\kappa^- - 1)]}, \tag{55}$$

whereas  $k_\theta$  remains unprescribed and neutrality is possible only for inclusions stiffer than the matrix,  $\mu^-/\mu^+ \geq 1$ . Assuming for simplicity  $\kappa^+ = \kappa^-$ , we report in Fig. 11 the regions in the plane  $\mu^-/\mu^+$  versus  $\delta/R$  where neutrality is possible (namely, when the

compliance parameter  $k$  of the continuous structural interface is positive), for two bar inclinations  $\alpha = 0$  and  $\pi/2$ . We note that all values of  $\mu^-/\mu^+$  lying above the curve marked  $\alpha = 0$  correspond to strong neutrality under equibiaxial stress (we mean therefore points in the light gray zone). Strong neutrality under equibiaxial remote stress for  $\alpha = \pi/2$  is possible at every point in the figure (thus in both the light and dark gray zones). Other values of  $\alpha$  have been investigated and they always correspond to limiting curves lying below the limiting curve for  $\alpha = 0$  shown in the figure. Therefore, for a circular inclusion coated by a continuous double Warren truss structure, differently from a linear zero-thickness interface, strong neutrality for equibiaxial tension is possible also for  $\mu^-/\mu^+ < 1$ .

- For remote shear stress, strong neutrality occurs when both  $B_m$  and  $M_m$  vanish, see Eq. (53). In particular, from the condition  $M_m = 0$  we obtain a linear equation in  $k$ , which can be solved as function of  $\mu^-/\mu^+$ . Introduction of this computed value into the equation  $B_m = 0$  yields a polynomial expression of second order for  $\mu^-/\mu^+$ . Assuming for simplicity  $\kappa^+ = \kappa^-$ , the values of the parameters  $\mu^-/\mu^+$  and  $\delta/R$  for which strong neutrality is possible for different values of bars' inclination  $\alpha$  are reported in Fig. 12. In the particular case of a linear zero-thickness interface, we obtain that neutrality is possible under shear for

$$k = \frac{2\mu^- \mu^+}{R(\mu^- - \mu^+)}, \quad \alpha = \frac{\pi}{4}, \tag{56}$$

so that  $k_r = k_\theta = k$ , a result coincident with that given by Ru (1998). Therefore, for a zero-thickness linear interface, the neutrality condition is possible only for inclusions stiffer than the matrix,  $\mu^-/\mu^+ \geq 1$ , whereas for a continuous structural interface this condition is not necessary if  $\alpha > \pi/3$ . In addition, we note from Fig. 12 that under remote shear stress, strong neutrality is possible only for  $\alpha \geq \pi/4$  (the case  $\alpha = \pi/4$  is attained in the limit case of a zero-thickness linear interface). It is interesting to observe that for  $\pi/3 < \alpha < \pi/2$ , strong neutrality is possible on two separate branches: (i) for  $\delta/R < 0.2$  with  $\mu^-/\mu^+ \geq 1$  and employing a continuous structural interface characterized by high stiffness  $k$ ; (ii) for  $\delta/R > 0.2$  also for inclusions less stiff than the matrix.

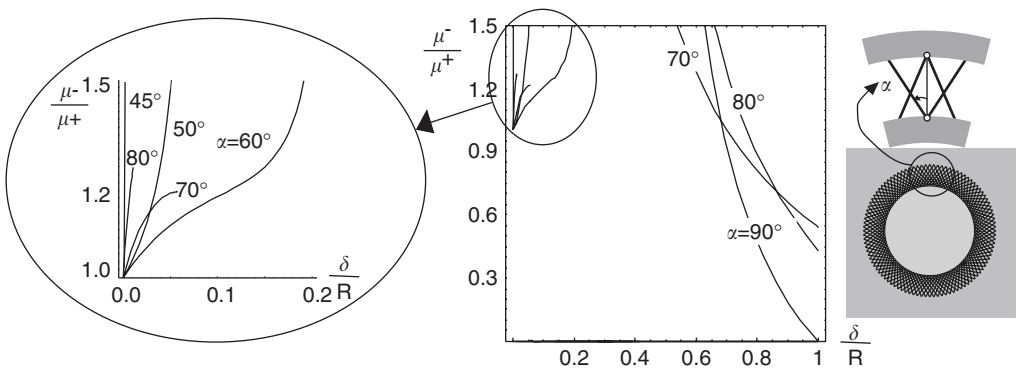


Fig. 12. Circular inclusion of radius  $R$  connected to an infinite matrix by a continuous double Warren truss structure of thickness  $\delta$  and bars inclination  $\alpha$ . Combinations of parameters  $\mu^-/\mu^+$ , and  $\delta/R$  for which strong neutrality is possible under remote shear stress, for different values of the bar inclination  $\alpha$ . Admissibility corresponds to all points on the curves.

- In closure, we emphasize that: *the range of parameters for which neutrality occurs for a continuous structural interface is much broader and extends to values  $\mu^-/\mu^+ < 1$  (inclusions less stiff than the matrix) than that obtained by employing the zero-thickness linear interface model (limited to inclusions stiffer than the matrix).*

### 3.3. Weak neutrality for an elliptical inclusion connected to an infinite matrix by a discrete structural interface

Let us consider an elliptical inclusion connected to an infinite matrix by a structural interface, so that we can make recourse to Eqs. (13), (15) and (23). Substituting these equations into the weak-neutrality condition (48) and employing the representation (50) yields the *condition of weak neutrality* in the same form (49), but with  $\mathbf{H}$  given now by

$$\begin{aligned}
 H_{11} &= [2 + m(-7 + 6m) + \kappa(2 + m - 2m^2)]\pi + \frac{(1 + \kappa)}{4\mu} \\
 &\quad \times \{ (3 - \kappa)[(m - 3)(a^{-(0,0)} + c^{-(0,0)}) + (1 - m)(b^{-(0,0)} + d^{-(0,0)})] \\
 &\quad + (\kappa(m + 2) - 2 - 3m)[(m - 3)(a^{+(0,0)} - c^{+(0,0)}) + (1 - m)(b^{+(0,0)} - d^{+(0,0)})] \}, \\
 H_{22} &= 16(\kappa - 1)\pi - \frac{4(\kappa^2 - 1)}{\mu} [a^{+(1,1)} + b^{+(1,1)} + c^{+(1,1)} + d^{+(1,1)}], \\
 H_{33} &= (2 + m(7 + 6m) - \kappa(m - 2 + 2m^2))\pi + \frac{(1 + \kappa)}{4\mu} \\
 &\quad \times \{ (3 - \kappa)[(m + 1)(a^{-(0,0)} + c^{-(0,0)}) - (3 + m)(b^{-(0,0)} + d^{-(0,0)})] \\
 &\quad + (\kappa(m - 2) + 2 - 3m)[(m + 1)(a^{+(0,0)} - c^{+(0,0)}) - (3 + m)(b^{+(0,0)} - d^{+(0,0)})] \}, \\
 H_{12} &= \frac{(1 + \kappa)}{2\mu} \{ (3 - \kappa)[a^{-(0,1)} + b^{-(0,1)} + c^{-(0,1)} + d^{-(0,1)}] \\
 &\quad + (1 - \kappa)(m - 3)(a^{+(1,0)} + c^{+(1,0)}) + (\kappa - 1)(m - 1)(d^{+(1,0)} + b^{+(1,0)}) \\
 &\quad + (\kappa(2 + m) - 2 - 3m)[a^{+(0,1)} + b^{+(0,1)} - c^{+(0,1)} - d^{+(0,1)}] \}, \\
 H_{13} &= 2[5 + 3m^2 - \kappa(m^2 + 3)]\pi + \frac{(1 + \kappa)}{4\mu} \\
 &\quad \times \{ (3 - \kappa)[(m - 1)(a^{-(0,0)} + c^{-(0,0)}) - (1 + m)(b^{-(0,0)} + d^{-(0,0)})] \\
 &\quad + [\kappa(4 - m + m^2) - 4 + 3m - 3m^2](a^{+(0,0)} - c^{+(0,0)}) \\
 &\quad - [\kappa(4 + m + m^2) - 4 - 3m - 3m^2](b^{+(0,0)} - d^{+(0,0)}) \}, \\
 H_{23} &= H_{12} + \frac{2(\kappa^2 - 1)}{\mu} [c^{+(0,1)} - c^{+(1,0)} - b^{+(0,1)} + b^{+(1,0)} + d^{+(0,1)} \\
 &\quad + d^{+(1,0)} - a^{+(0,1)} - a^{+(1,0)}],
 \end{aligned} \tag{57}$$

where

$$\begin{aligned}
 a^{\pm(i,g)} &= \sum_{k,j=1}^N A_{jk} \cos\left(\hat{\theta}_k^{\pm} + i\frac{\pi}{2}\right) \cos\left(\beta_j + g\frac{\pi}{2}\right), \\
 b^{\pm(i,g)} &= \sum_{k,j=1}^N B_{jk} \cos\left(\hat{\theta}_k^{\pm} + i\frac{\pi}{2}\right) \sin\left(\beta_j - g\frac{\pi}{2}\right), \\
 c^{\pm(i,g)} &= \sum_{k,j=1}^N C_{jk} \sin\left(\hat{\theta}_k^{\pm} - i\frac{\pi}{2}\right) \cos\left(\beta_j + g\frac{\pi}{2}\right), \\
 d^{\pm(i,g)} &= \sum_{k,j=1}^N D_{jk} \sin\left(\hat{\theta}_k^{\pm} - i\frac{\pi}{2}\right) \sin\left(\beta_j - g\frac{\pi}{2}\right).
 \end{aligned} \tag{58}$$

If the structural interface is symmetric with respect to both  $x_1$  and  $x_2$  axes

$$\begin{aligned}
 a^{\pm(0,1)} &= b^{\pm(0,1)} = c^{\pm(0,1)} = d^{\pm(0,1)} = 0, \\
 a^{\pm(1,0)} &= b^{\pm(1,0)} = c^{\pm(1,0)} = d^{\pm(1,0)} = 0,
 \end{aligned} \tag{59}$$

so that

$$H_{12} = H_{23} = 0, \tag{60}$$

a condition which thoroughly simplifies the calculations. For the particular case of a structural interface symmetric with respect to both  $x_1$  and  $x_2$  axes, we can compute the eigenvalues  $h_i$  and the corresponding eigenvectors  $\mathbf{v}_i$  of the matrix  $\mathbf{H}$ , which turn out to be

$$\begin{aligned}
 h_1 &= H_{22}, & \mathbf{v}_1 &= [0, 1, 0]^T \\
 h_2 &= \frac{H_{11} + H_{33} - \sqrt{\Delta}}{2}, & \mathbf{v}_2 &= \left[ \frac{H_{11} - H_{33} - \sqrt{\Delta}}{2H_{13}}, 0, 1 \right]^T, \\
 h_3 &= \frac{H_{11} + H_{33} + \sqrt{\Delta}}{2}, & \mathbf{v}_3 &= \left[ \frac{H_{11} - H_{33} + \sqrt{\Delta}}{2H_{13}}, 0, 1 \right]^T,
 \end{aligned} \tag{61}$$

with  $\Delta = 4H_{13}^2 + (H_{11} - H_{33})^2$ . Therefore

*assuming  $H_{13}(H_{11} - H_{33}) \neq 0$ , the inclusion can be weakly neutral only when a uniform shear is applied at infinity and no neutrality under equibiaxial stress is found.*

Although we cannot exclude that either  $H_{11} = H_{33}$  or  $H_{13} = 0$  might be satisfied, we were unable to find a geometry for the interfacial structure to satisfy such a condition for an elliptical inclusion (in contrast to the circular case), so that we were unable to find weak neutrality under biaxial stress for elliptical inclusions or reinforced voids.

As an example, an elliptical void with  $a/b = 5$  is considered, reinforced with 15 double Warren truss structural elements comprised of bars with thickness  $t_b/a = \frac{1}{1000}$ , as shown in Fig. 13. The infinite matrix is characterized by  $\nu = \frac{1}{3}$  and loaded by a uniform remote shear stress  $\sigma_{12}^{\infty} = \mu/100$ . The bars' stiffness is selected to satisfy the weak neutrality condition given by Eq. (48) and corresponding to  $\Delta = 0.17$ . It is clear from Fig. 13, where the absolute value of the components of stress perturbation (normalized by the remote shear stress, i.e.  $|\sigma_{ij} - \sigma_{ij}^{\infty}|/\sigma_{12}^{\infty}$ ) are shown, that, when the elliptical void is weakly neutral, the perturbation introduced is very localized near the bar junctions, whereas the perturbation

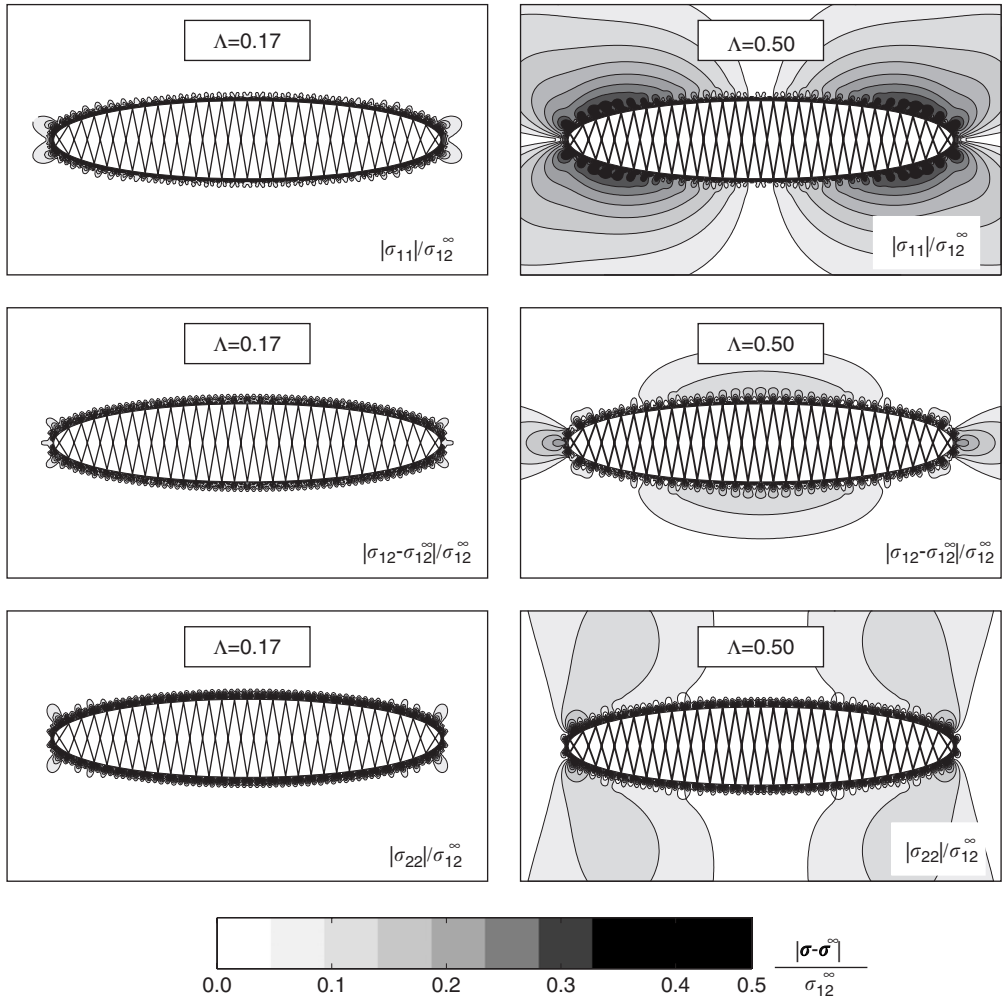


Fig. 13. Elliptical void reinforced by 15 double Warren truss structures and loaded by a remote shear stress: weak neutrality occurs for bars compliance  $\Lambda = 0.17$ , so that in this case the stress fields are almost unperturbed (compare to the non-neutral case  $\Lambda = 0.5$ ). Maps of the absolute values of the perturbation in the stress components (normalized by the remote stress) are shown.

spreads through the matrix when the bar stiffness is changed (see the other example with  $\Lambda = 0.5$ ).

3.3.1. Weak neutrality for a circular inclusion reinforced by a discrete structural interface

Let us consider a circular inclusion having radius  $R$  connected to an infinite matrix with a circular hole of radius  $R + \delta$  by a structural interface. For this particular geometry  $m = 0$ ,  $\theta_k^n = \beta_k = \theta_k$ ,  $\hat{\theta}_k^+ = 2\theta_k$  and  $\hat{\theta}_k^- = 0$ , so that

$$\begin{aligned}
 a^{-(1,0)} &= a^{-(1,1)} = 0, & b^{-(1,0)} &= b^{-(1,1)} = 0, \\
 c^{-(0,0)} &= c^{-(0,1)} = 0, & d^{-(0,0)} &= d^{-(0,1)} = 0.
 \end{aligned}
 \tag{62}$$

Therefore, coefficients (57) for the particular case of a structural interface symmetric with respect to both  $x_1$  and  $x_2$  axes simplify to

$$\begin{aligned}
 H_{11} &= 2\pi(1 + \kappa) + \frac{1 + \kappa}{4\mu} \{(3 - \kappa)(b^{-(0,0)} - 3a^{-(0,0)}) \\
 &\quad + 2(\kappa - 1)[b^{+(0,0)} - d^{+(0,0)} - 3(a^{+(0,0)} - c^{+(0,0)})]\}, \\
 H_{22} &= 16\pi(\kappa - 1) - \frac{4(\kappa^2 - 1)}{\mu} (a^{+(1,1)} + b^{+(1,1)} + c^{+(1,1)} + d^{+(1,1)}), \\
 H_{33} &= 2\pi(1 + \kappa) + \frac{1 + \kappa}{4\mu} \{(3 - \kappa)(a^{-(0,0)} - 3b^{-(0,0)}) \\
 &\quad + 2(\kappa - 1)[c^{+(0,0)} - a^{+(0,0)} - 3(d^{+(0,0)} - b^{+(0,0)})]\}, \\
 H_{13} &= 2\pi(5 - 3\kappa) + \frac{1 + \kappa}{4\mu} [(\kappa - 3)(a^{-(0,0)} + b^{-(0,0)}) \\
 &\quad + 4(\kappa - 1)(a^{+(0,0)} - b^{+(0,0)} - c^{+(0,0)} + d^{+(0,0)})], \\
 H_{23} &= H_{12} = 0.
 \end{aligned} \tag{63}$$

If the structure is symmetric about  $n$  distinct diametral lines at fixed angles  $2\pi/n$ , we find that, in addition to Eqs. (58) we have

$$\begin{aligned}
 a^{-(0,0)} &= b^{-(0,0)}, \\
 a^{+(0,0)} &= a^{+(1,1)} = -b^{+(0,0)} = b^{+(1,1)}, \\
 d^{+(0,0)} &= d^{+(1,1)} = -c^{+(0,0)} = c^{+(1,1)},
 \end{aligned} \tag{64}$$

so that Eqs. (63) reduce to

$$\begin{aligned}
 H_{11} &= H_{33} = 2(1 + \kappa)\pi + \frac{1 + \kappa}{2\mu} [(\kappa - 3)a^{-(0,0)} + 4(1 - \kappa)(a^{+(0,0)} - c^{+(0,0)})], \\
 H_{13} &= (\kappa - 3) \left[ -4\pi + \frac{\kappa + 1}{\mu} a^{-(0,0)} \right] - H_{11}, \\
 H_{12} &= H_{23} = 0, \quad H_{22} = 2(H_{11} - H_{13}).
 \end{aligned} \tag{65}$$

For this particular case, the eigenvalues  $h_i$  and the corresponding eigenvectors  $\mathbf{v}_i$  of the matrix  $H$  turn out to be

$$\begin{aligned}
 h_1 &= H_{11} + H_{13}, \quad \mathbf{v}_1 = [1, 0, 1]^T, \\
 h_2 &= h_3 = H_{22}, \quad \mathbf{v}_2 = \mathbf{v}_3 = [0, 1, 0]^T,
 \end{aligned} \tag{66}$$

showing that now weak neutrality is possible for shear and equibiaxial stress separately. It follows that for a circular inclusion connected to an infinite matrix by a (symmetric, discrete) structural interface, neutrality occurs:

- for remote equibiaxial tension when

$$H_{11} + H_{13} = (\kappa - 3) \left[ 4\pi - \frac{\kappa + 1}{\mu} a^{-(0,0)} \right] = 0 \implies a^{-(0,0)} = \frac{4\mu\pi}{1 + \kappa}. \tag{67}$$

- for remote shear stress when

$$\begin{aligned}
 H_{22} &= (\kappa - 1) \left[ 2\pi - \frac{\kappa + 1}{\mu} (a^{+(0,0)} - c^{+(0,0)}) \right] = 0 \\
 \implies a^{+(0,0)} - c^{+(0,0)} &= \frac{2\mu\pi}{1 + \kappa}.
 \end{aligned}
 \tag{68}$$

As already observed in the case of a circular inclusion coated by a continuous double Warren truss structure, Eq. (67) is also satisfied for a matrix characterized by  $\kappa = 3$  (i.e.  $\nu = 0$ ) and Eq. (68) for a matrix characterized by  $\kappa = 1$  (i.e.  $\nu = \frac{1}{2}$ ). However, for these cases higher-order terms should be considered in the series expansion of the energy.

As an example of weak neutrality, a circular inclusion with a 30-cell hexagonal lattice structural interface comprised of bars with thickness  $t_b/R = \frac{1}{1000}$  is considered, with an inclusion radius  $R$  and a thickness of the structure  $\delta = R/4$  (Fig. 14). The two materials forming the inclusion and the matrix are characterized by the same value of Poisson ratio  $\nu = \frac{1}{3}$  and by  $\mu^-/\mu^+ = 10$ , so that the inclusion is stiffer than the matrix. A remote shear loading ( $\sigma_{12}^\infty = \mu^+/100$ ) is applied, so that the condition of weak neutrality (68) is achieved for  $\Lambda = 0.52$ . As a comparison, the (non-neutral) value  $\Lambda = 0.15$  is investigated. The level sets of the absolute value of the components of stress perturbation (normalized by the

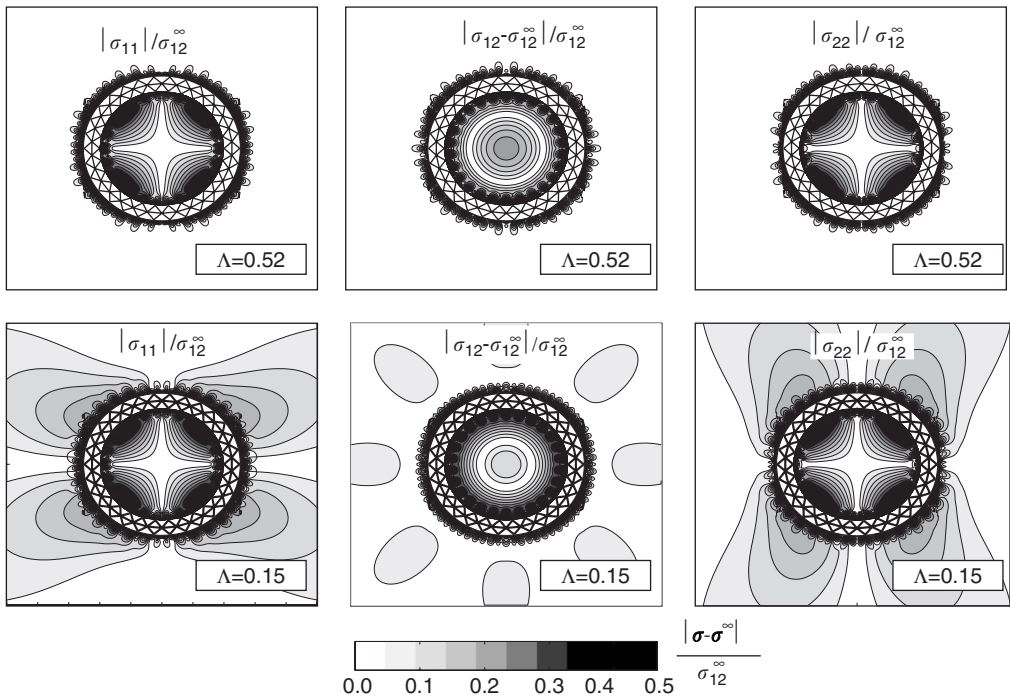


Fig. 14. Circular inclusion connected to an infinite matrix by a 30-cell hexagonal lattice structure and loaded by a remote shear stress: weak neutrality occurs for the bars compliance  $\Lambda = 0.52$  (upper part), so that in this case the stress fields are almost unperturbed (compare to the non-neutral case  $\Lambda = 0.15$ ). Maps of the absolute values of the perturbation in the stress components (normalized by the remote stress) are shown. The inclusions are stiffer than the matrix ( $\mu^-/\mu^+ = 10$ ) and  $\nu^+ = \nu^- = \frac{1}{3}$ .

remote shear stress, i.e.  $|\sigma_{ij} - \sigma_{ij}^{\infty}|/\sigma_{12}^{\infty}$ ) are shown in Fig. 14, again illustrating that, when the inclusion is weakly neutral, the perturbation introduced in the matrix is minimal.

#### 4. Conclusions

We have shown that the model of a structural interface developed in Part I of this article is a powerful tool to investigate different situations of interest related to inclusions coated with structures: (i) effective properties, and (ii) stress neutrality. In particular, we have determined for the first time:

- The effective properties of a dilute suspension of randomly oriented bridged elliptical voids and bridged elliptical inclusions.
- A new, weak neutrality condition that can be satisfied for inclusions coated with a structural interface.

The tools developed allow design of interfacial structures to obtain optimal properties, which have been in part explored, providing for instance the structures shown in Fig. 5 giving the maximal effective properties of a composite containing reinforced circular inclusions.

#### Acknowledgments

Financial support of MURST-Cofin 2003 (prot. 2003082105\_002) (K.B. and D.B.) is gratefully acknowledged. Part of this research was performed while D.B. was visiting professor at the Department of Engineering Physics at the University of Wisconsin (Madison, USA), which hospitality is gratefully acknowledged. W.J.D. acknowledges support from Italian Ministry Research Grant “Rientro dei cervelli MIUR 26/1/2001” and from Lawrence Livermore National Laboratories under Contract W-7405-Eng-48 with the US Department of Energy.

#### References

- Achenbach, J.D., Zhu, H., 1989. Effect of interfacial zone on mechanical behavior and failure of fiber-reinforced composites. *J. Mech. Phys. Solids* 37, 381–393.
- Achenbach, J.D., Zhu, H., 1990. Effect of interphases on micro and macromechanical behavior of hexagonal-array fiber composites. *J. Appl. Mech.* 57, 956–963.
- Benveniste, Y., 1985. The effective mechanical behavior of composite materials with imperfect contact between the constituents. *Mech. Mater.* 4, 197–208.
- Bigoni, D., Movchan, A.B., 2002. Statics and dynamics of structural interfaces in elasticity. *Int. J. Solids Struct.* 39, 4843–4865.
- Bigoni, D., Serkov, S.K., Movchan, A.B., Valentini, M., 1998. Asymptotic models of dilute composites with imperfectly bonded inclusions. *Int. J. Solids Struct.* 35, 3239–3258.
- Hashin, Z., 1990. Thermoelastic properties of fiber composites with imperfect interface. *Mech. Mater.* 8, 333–348.
- Hashin, Z., 1991a. The spherical inclusion with imperfect interface. *J. Appl. Mech.* 58, 444–449.
- Hashin, Z., 1991b. Thermoelastic properties of particulate composites with imperfect interface. *J. Mech. Phys. Solids* 39, 745–762.
- Hashin, Z., 2002. Thin interphase/imperfect interface in elasticity with application to coated fiber composites. *J. Mech. Phys. Solids* 50, 2509–2537.
- Jasiuk, I., Chen, J., Thorpe, M.F., 1994. Elastic moduli of two dimensional materials with polygonal and elliptical holes. *Appl. Mech. Rev.* 47, S18–S28.

- Kachanov, M., Tsukrov, I., Shafiro, B., 1994. Effective moduli of solids with cavities of various shapes. *Appl. Mech. Rev.* 47, S151–S174.
- Levy, A.J., 1996. The effective dilational response of fiber-reinforced composites with non linear interface. *J. Appl. Mech.* 63, 357–364.
- Milton, G.W., Serkov, S.K., 2001. Neutral coated inclusions in conductivity and anti-plane shear. *Proc. R. Soc. London A* 457, 1973–1997.
- Ru, C.Q., 1998. Interface design of neutral elastic inclusions. *Int. J. Solids Struct.* 35, 559–572.
- Thorpe, M.F., Jasiuk, I., 1992. New results in the theory of elasticity for two-dimensional composites. *Proc. R. Soc. London A* 438, 531–544.
- Thorpe, M.F., Sen, P.N., 1985. Elastic moduli of two-dimensional composite continua with elliptical inclusions. *J. Acoust. Soc. Am.* 77, 1674–1680.
- Walpole, L.J., 1978. A coated inclusion in an elastic medium. *Math. Proc. Cambridge Phil. Soc.* 83, 495–506.
- Willis, J.R., 1982. Elasticity theory of composites. In: Hopkins, H.G., Sewell, M.J. (Eds.), *Mechanics of Solids, The Rodney Hill 60th Anniversary Volume*. Pergamon, Oxford, pp. 653–686.